

## 2. BLOCK COPOLYMER SYNTHESIS & MICROPHASE SEPARATION

### 2.1. Introduction

Among the most important aspects of template directed alignment of nanoparticles is the preparation of a templating medium with properties suitable for use with the nanoparticles in question. Of particular importance in this work is the formation of a *block copolymer* template with microphases sufficiently large to selectively sequester the segmented nanorods that are to be assembled; the acquisition of such large microphases being typically rather difficult to achieve. In order to prepare such a template, it is important to first make a number of decisions with regards to the template properties and from there, the method of template preparation. In this work, the first such decision is the selection of the block copolymer system that is to be used, as this will determine the properties of the nanoparticle template. Based on this system, a *series* of block copolymer templates with variations in key properties will be prepared, in an effort to identify the critical parameters in achieving the research objective. The block copolymer system used in this work (and the parameters that are varied) is selected on the basis of the following considerations.

#### Block Copolymer Selection

Firstly, it is important to determine what microphase morphologies are desired, as this dictates the number of blocks and block volume fractions that are necessary. In this work, diblock copolymers with lamellar and spherical morphologies are targeted. A diblock copolymer is chosen in order to simplify the block copolymer synthesis and provide relatively simple to examine microphase structures, as only two microphases are present. The lamellar and spherical morphologies are selected so that the influence of interface curvature

(and consequently the differences in the degree of chain stretching required at the interface to accommodate the nanorods) upon the cross-phase templating may be investigated.

The second consideration is the total molecular weight of the block copolymer, as this effectively determines the size of the microphases. In order for the block copolymer microphases to effectively direct the alignment of the nanorods, microphases with dimensions greater than those of the nanorods are required. Considering the use of free nanorods with segment diameters and lengths at the lower limits of that which can be reasonably synthesised with available templates and electrochemistry apparatus (as discussed in the chapter on single segment nanorods), this means that lamellae 50nm thick and spheres 40nm in diameter or greater are required. For a typical block copolymer, this requires controlled molecular weights  $\geq 250\text{kg/mol}$ , which is relatively hard to synthesise (typically requires ionic polymerisation techniques) and process (difficult to melt or dissolve for microphase separation). An alternative means of achieving these microphase dimensions is to utilise block copolymers with lower molecular weights, and swell the microphase domains with highly selective non-volatile solvents in order to increase their volume. The inclusion of any solvent to a block copolymer will scale the microphase dimensions by the following factor: [1]

$$d \sim \Phi_p^{-\beta}$$

where  $\Phi_p$  is the volume fraction of the copolymer block being swelled. Neutral (non-selective) solvents have negative values of  $\beta$  (corresponding to shielding by the solvent of the repulsion between dissimilar blocks) which leads to an effective reduction in microphase size, whereas selective solvents can have positive values of  $\beta$  which leads to increases in the microphase dimensions when swelled with these solvents. [1] Different solvent/block copolymer combinations result in different  $\beta$  values, with the largest values resulting from the use of homopolymers (corresponding to the blocks in the copolymer) as the highly selective “solvent”. [1] The effectiveness of this

method of increasing the microphase dimensions also depends upon a number of other factors. For example, the effect of swelling is increased when the swelled block constitutes a minority of the block copolymer volume, although increasing the minority blocks effective volume fraction may also lead to a phase transition to a different microphase morphology at sufficiently high volume fractions of solvent, due to increased stretching of the chains. In some work, this has actually been exploited to achieve large increases in microphase size, by swelling the minority block to the extent that a mirror image morphology is generated i.e. an AB diblock copolymer with A block cylinders in a B block matrix morphology becomes an A block matrix containing B block cylinders. [1] It has also been observed that greater dilutions result in a greater increase in microphase size. However, this is limited to a certain extent by the macrophase separation of the solvent from the block copolymer that occurs at high volume fractions of solvent. An additional factor is temperature, which plays a significant role in scaling the value of  $\beta$ . [1]

Based on this, the most commonly used selective solvent is homopolymer corresponding to the copolymer block to be swelled, as the high  $\beta$  values minimise the required volumes of homopolymer necessary to achieve a given microphase size, thereby minimising the possibility of macrophase separation or microphase transition. However, the use of homopolymer as a selective solvent introduces a number of other considerations, principally concerning the homopolymer molecular weight relative to that of the swelled copolymer block. For example, theoretical and experimental work indicates that generally,  $\beta$  decreases systematically with molecular weight [1-2] to the extent that if the homopolymer has a molecular weight below 1/10 of the corresponding copolymer blocks molecular weight,  $\beta$  is effectively zero (no effect). [1] Although, other research has suggested that this is not necessarily the case if homopolymers are used to swell all of the domains, not just the domain of interest. [3] The solubility of the homopolymer in the block copolymer follows an opposing trend. For example, when the ratio  $M_H/M_B$  between homopolymer molecular weight ( $M_H$ ) and the block to be swelled ( $M_B$ ) is very small, the homopolymer is significantly more soluble (a greater volume % can be added before macrophase separation occurs) than when this

ratio is larger. [4] At ratios of  $M_H/M_B > 1$ , the homopolymer is no longer soluble in the block copolymer and macrophase separation occurs. [5] Note however that a much higher solubility limit (minimum volume of homopolymer of a given molecular weight relative to the copolymer block that is added for macrophase separation to take place) can be achieved by introducing, and increasing the strength of, specific interactions between the solvent and solute. [6]

The balance between these two factors means that only moderate increases in microphase dimensions can be achieved by swelling before a microphase transition (unless all microphases are being swelled equally) or a macrophase transition occurs, after which no further increases in polymer microphase size takes place. Although this swelling method is generally useful for many applications, in order to achieve the large microphases desired for this work, a relatively high molecular weight block copolymer is still initially required before swelling.

The final element, the block composition, is dictated by two principal factors. The first of these is the availability of synthetic methods for a given combination of polymer blocks. In a typical block copolymer synthesis, the first copolymer block is produced with end functionality such that it can act as a “macro-initiator” in a subsequent polymerisation using a different monomer to form the second block. However, differences in chemical reactivity and required polymerisation mechanisms and conditions mean that not all macro-initiators are suitable for use in chain extension reactions with any given monomer. As such, the composition of the first and second blocks must be chosen to ensure that this chain extension can occur.

The second factor to consider is the thickness of the interface between the block copolymer microphases. It is anticipated that our synthesised nanorods will exhibit at least some variation in segment length within any given batch; a result of small differences between the pore diameters, the applied potential and the mass transport within each membrane. [7-8] Therefore, it may be desirable to have a block copolymer where the interfacial thickness (a region between pure microphases where there is a composition gradient) is relatively large, in order to compensate for this variation. However, a larger interfacial

thickness may in fact inhibit templating of the nanoparticle structure, by providing less selective interaction between the segmented nanorods and the copolymer blocks (fig 2.1). Thus, given that interfacial thickness is dictated by the Flory-Huggins interaction parameter [9-10], two block copolymer compositions with very different interaction parameters will be selected to study the effect of differences in the interfacial thickness (if any) to the templated alignment of segmented nanorods. One possible concern with using a block copolymer having a relatively small interaction parameter is that an even higher molecular weight than is typically required will be necessary to achieve the desired microphase dimensions, which also depend upon this parameter. However, given the high targeted molecular weights, these copolymer blocks will both be well into the strong segregation regime, so differences in the interaction parameters are expected to have only a very small effect on the domain sizes.

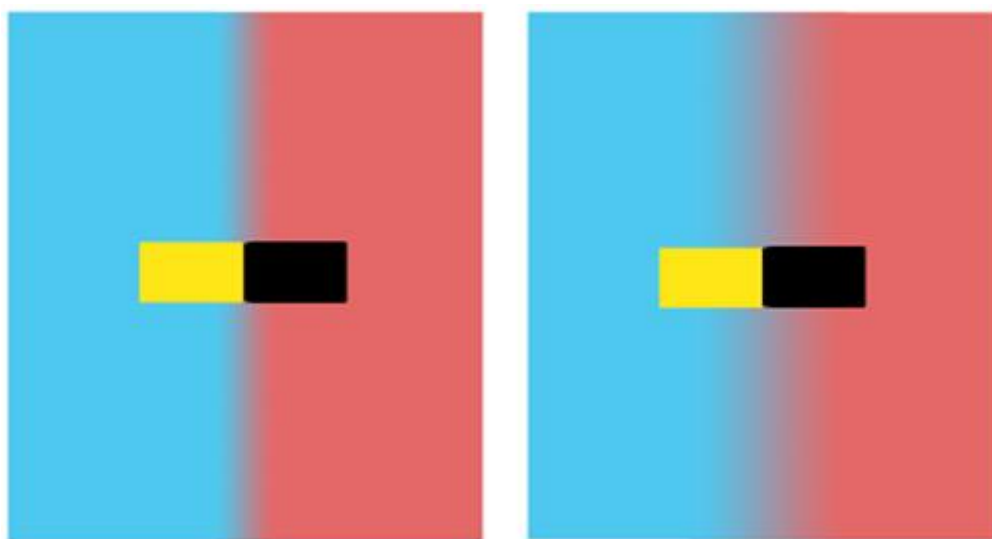


**Fig 2.1:** Depiction of a functionalised bi-segmented nanorod sequestered at the interface between two lamellar microphases with (left) a thin interface and (right) a thick interface.

Based on all of these these considerations, lamellar (50/50 vol%) and spherical (10/90 vol%) morphologies of the diblock copolymers Poly(styrene)-b-Poly(2-vinyl pyridine) (PS-b-P2VP) and Poly(methyl methacrylate)-b-Poly(n-butyl methacrylate) (PMMA-b-PBMA) with total molecular weights greater than 280kg/mol (lamellar) / 200kg/mol (spherical) and 320kg/mol (lamellar) / 250kg/mol (spherical) respectively (data used in

determining the required molecular weights is presented in table 2.1) are selected for use as nanoparticle templates. PS-b-P2VP was selected based on the number of studies which investigated the behaviour of this polymer in the template directed positioning of nanoparticles into individual phases [11-14] in addition to having a large interaction parameter. PMMA-b-PBMA was then chosen for its smaller interaction parameter (yielding a PMMA-b-PBMA domain interface thickness 1.85 times greater than for PS-b-P2VP). Both of these polymers are also advantageous in that they have well established microphase separation behaviour [15-16], and relatively simple staining techniques exist for the study of their microphase structures by transmission electron microscopy (TEM).

**Table 2.1:** Data related to the determination of equilibrium microphase periodicity relative to total degree of polymerisation for a diblock copolymer.

Polymer block	Flory- Huggins Interaction Parameter, $\chi$	Statistical Segment Length (nm)	Density (g/cm <sup>3</sup> )
PS	0.2124 (with P2VP) <sup>a</sup>	0.67 <sup>c</sup>	1.05
P2VP	""	0.67 <sup>d</sup>	1.146
PMMA	0.062 (with PBMA) <sup>b</sup>	0.71 <sup>e</sup>	1.19
PBMA	""	0.84 <sup>f</sup>	1.055

<sup>a</sup> [15], <sup>b</sup> [16], <sup>c</sup> [17-18], <sup>d</sup> [19], <sup>e</sup> [20], <sup>f</sup> [21]

### Synthesis

The second decision that needs to be made regards what synthesis method is to be used to produce the block copolymers. Although there exists a large number of methods that have been successfully applied to the controlled synthesis of both PMMA-b-PBMA and PS-b-P2VP, the synthesis of these polymers in this case is complicated by the fact that relatively high molecular weights with low polydispersity and active chain ends are required.

Traditionally, such high molecular weight block copolymers are synthesised using ionic polymerisation techniques, where the incidence of termination reactions is minimal. However, such techniques require very stringent reaction conditions, reagent purity and specialised equipment, making this process

difficult, costly and time intensive. Therefore, it is desirable to use other living polymerisation methods for the synthesis of these polymers where possible.

In the case of PS-*b*-P2VP, it turns out that the only effectively applied synthesis method developed to date that yields even moderately high molecular weight with low polydispersity is anionic polymerisation. \* Given that the required resources are not available to carry out this synthesis, this polymer was prepared elsewhere for use in this study (see section 2.2.1). The preparation of low polydispersity, high molecular weight PMMA-*b*-PBMA on the other hand, may be performed using ATRP. ATRP has already been shown to be amenable to the controlled synthesis of relatively high molecular weight methacrylate homopolymers [22-30], and it remains possible that ATRP may be optimised here for the synthesis of methacrylate based *block copolymers* with controlled polymer growth to even higher molecular weights, by using a number of recommendations made in the literature towards further reducing the incidence of termination reactions. [31] The fraction of terminated polymer chains in ATRP is higher in reactions involving high rates of polymerisation, high monomer conversions, low initiator concentrations and high ratios of termination to propagation rates ( $k_t/k_p^2$ ). [32] Thus by adjusting these factors, the fraction of terminated polymer chains may be minimised. The polymerisation rate, for example, may be reduced by decreasing the reaction temperature, or by decreasing the concentration of propagating polymer radicals. This decrease in concentration may be accomplished through the use of a catalyst system where the equilibrium strongly favours deactivated over activated polymer chains or through dilution with an appropriate solvent; although this dilution will also serve to reduce initiator concentration. Lower monomer conversions (C) for a target polymer molecular weight ( $M_n$ ) may be achieved by increasing the monomer to initiator ratio ( $[M]/[I]$ ), as the theoretical molecular weight ( $M_n$ ) is determined by the product of these two parameters. [24]

---

\* Note that commonly used alternative high molecular weight polymers with large interaction parameters (such as Poly(styrene)-*b*-Poly(isoprene)) are also generally restricted to synthesis by living ionic techniques.

$$Mn = \frac{[M]}{[I]} \cdot C \cdot M_{monomer}$$

However, this also leads to an overall decrease in initiator concentration, so a balance between these factors is required. [33]

The ratio of termination to propagation reaction rates can be varied in a number of ways. One way involves decreasing the diffusion rate of the growing polymer chains relative to the monomer species in the polymerisation medium, which serves to reduce the rate of termination relative to propagation. [34] This may be achieved by polymerising to higher monomer conversions to increase solution viscosity (undesirable as it increases the fraction of terminated polymer chains by other mechanisms), polymerising to higher chain lengths (which limits polymer chain diffusion), by lowering the temperature or by using a solvent with higher viscosity than the monomer. [34] Interestingly, increasing the temperature can also act to decrease this ratio, as the activation energy of propagation is much higher than that of termination. This is offset by the domination of chain transfer reactions at these higher temperatures, which have even higher activation energy. [32] A further way of reducing this ratio is to increase the pressure in the reaction vessel, as the volume of activation for radical propagation is negative while for termination it is positive. [31, 35-38] However, this requires the use of specialised reaction vessels. Clearly, many of these parameters affect the polymerisation system in a number of interrelated ways, therefore the reaction conditions must be chosen carefully in order to minimise termination reactions.

In this work, the polymerisation system that is selected for optimisation is the ATRP of PMMA using a Copper Bromide (CuBr) / N, N, N', N'', N'''-Pentamethyldiethylenetriamine (PMDETA) catalyst complex and Ethyl 2-bromoisobutyrate as the initiator (mole ratio of [EBrIB]:[CuBr]:[PMDETA] is 1:1:1), which is subsequently used as a macro-initiator in chain extension with nBMA using a Copper Chloride (CuCl) / PMDETA catalyst complex (mole ratio of [PMMA-Br]:[CuCl]:[PMDETA] is 1:1:1). This system was selected as it has previously been shown to be suitable for the synthesis of moderately



high molecular weight PMMA-b-PBMA block copolymers with low polydispersity [39], arising from (i) the relatively low propagating radical concentration (equilibrium favours dormant chains therefore fewer termination reactions), (ii) its tendency to undergo very few side reactions (as its catalyst remains available to activate/deactivate chains throughout the whole polymerisation) [40-41] and (iii), its high initiation efficiency (fast initiation relative to propagation and termination [29, 42]) of the initiators used. This high initiation efficiency results from both the highly labile C-Br initiator bond relative to the dormant polymer species [43], and the use of so called “halogen exchange” with a CuCl catalyst in the chain extension reaction [42], where the polymer chains undergoing chain extension are converted from an initiating R-Br dormant form (as is the case for the macro-initiator) to the less reactive R-Cl dormant form following initiation. [44-46] By replacing Br with Cl after initiation, the rate of propagation (less labile R-Cl species) is reduced relative to initiation (more labile R-Br species), helping to maintain a low polydispersity. The reduced rate of propagation of the R-Cl species will also contribute towards a reduction in the extent of termination reactions. An additional advantage of this polymerisation system is that the catalyst complex is cheap, readily available [40-41] and can also be removed from the polymer end product using a simple filtration process. [47-49]

The selected system is optimised for controlled high molecular weight polymerisation through the use of moderate reaction temperatures (to ensure there is sufficient activation energy for propagation but not enough for disproportionation: 90°C has been found to be optimal for this system) [50-51] and moderate dilution with methoxybenzene (typically 50% v/v is used [51]) to maintain a low polymer radical concentration throughout the reaction, whilst allowing solution viscosity to increase with monomer conversion. This particular solvent was selected as the polymer is soluble in methoxybenzene and it does not negatively affect the catalyst system used or introduce significant chain transfer reactions. [52-55] Methoxybenzene also has the benefit of improving the catalyst complex solubility [30, 44, 50], which acts to improve the efficiency of polymer chain activation/deactivation, thereby promoting a low polydispersity. [56]

The number of termination reactions can be minimised in order to obtain a high molecular weight polymer by striking a balance between monomer conversion and the monomer to initiator ratio; as large values for either of these parameters contribute towards high degrees of termination (thereby preventing controlled polymerisation up to high molecular weight) while low values restrain the maximum molecular weight that may be obtained. However, as the optimal balance between these two parameters varies between systems, initial work in optimising the macroinitiator polymerisation system uses relatively modest monomer/initiator ratios. The system is then studied to determine the monomer conversions at which termination becomes significant. From there, further adjustments to the monomer/initiator ratio and target monomer conversion may be made to maximise the controlled molecular weight. This process is then repeated with chain extension in order to obtain a controlled, high molecular weight block copolymer.

It is important to note that while other ATRP systems have been shown to be able to access much higher molecular weights with low polydispersity, the conditions used in these systems are generally optimised for the synthesis of high molecular weight homopolymers, such that termination reactions become prevalent towards the end of the polymerisation, thereby making them unsuitable for use as macroinitiators in the synthesis of block copolymers. [23, 26, 30, 57] Furthermore, many of these other methods involve specialised glassware (polymerisation in vacuum) and costly reagents. The selected system, on the other hand, is conducted under nitrogen atmosphere, using readily available and easy to purify reagents and a simple apparatus.

### Microphase Separation

The final decision that needs to be made is on the method by which microphase separation will be carried out. Given the high target molecular weight of the block copolymers, microphase separation through raising the temperature may be problematic due to thermal degradation of the polymer prior to melting. [58] On the other hand, such high molecular weight PMMA-b-PBMA [59] and PS-b-P2VP [14] are soluble in non-selective organic

solvents. Therefore, microphase separation by dissolution in a non-selective solvent followed by slow evaporation of the solvent will be used to obtain essentially equilibrium microphase separated block copolymer samples. It should be noted however, that slow evaporation alone will not be sufficient to achieve *complete* thermodynamic equilibrium (and therefore the largest possible domain sizes), as the polymer chains are kinetically constrained from undergoing further rearrangement of their configurations below a particular solvent content. In order to achieve complete thermodynamic equilibrium chain configurations, slow evaporation of the solvent is followed by vacuum evaporation of residual trapped solvent in the polymer at temperatures higher than the polymer blocks glass transition temperatures. When completed, the desired limited rearrangement of polymer chains should occur. [59-61]

### Summary

The aim of the work covered in this chapter is to prepare a series of block copolymers with variation in several important template controlled parameters. These block copolymers will be used as templates to investigate their influence on nanoparticle alignment. The template controlled parameters varied include the microphase interface curvature (lamellar vs. spherical microphase morphologies) and interfacial thickness (high vs. low Flory interaction parameters). In order to obtain domains large enough to accommodate the nanorods, controlled synthesis of very high molecular weight polymers is necessary, which is typically rather difficult. A high  $\chi$  polymer, PS-*b*-P2VP, is synthesised by anionic polymerisation while a low  $\chi$  polymer, PMMA-*b*-PBMA, is formed by ATRP which is optimised to further reduce termination reactions so as to achieve the controlled high molecular weights needed in this study. The resulting polymers are characterised to ensure they are suitable for use as nanoparticle templates. Finally, the block copolymers will be microphase separated using an established procedure, and the resulting morphology examined to confirm the suitability of the block copolymers for use as nanoparticle alignment templates.

## 2.2. Experimental Method & Materials

### 2.2.1. Synthesis of PS-b-P2VP

Lamellar PS-b-P2VP with a molecular weight of (190000)-b-(190000) g/mol (block ratio of ~50:50 vol%) and PDI of 1.1 was bought from Polymer Source inc. (Quebec, Canada) while spherical PS-b-P2VP with a molecular weight of (30000)-b-(410000) g/mol (block ratio of ~10:90 vol%) was synthesised by David Uhrig (CNMS, Oak Ridge National Laboratory, USA) by sequential living anionic polymerisation in THF at -78°C.

### 2.2.2. Synthesis of PMMA-b-PBMA

#### Monomer Purification

Prior to polymerisation, the monomer (Aldrich, 99%) is treated by stirring over CaH<sub>2</sub> (1g / 100ml monomer) overnight to remove water from the monomer. The monomer is then filtered and eluted through a column of activated basic alumina (to remove the polymerisation inhibitor Methylethylhydroxyquinone, MEHQ) followed by distillation in vacuo to separate the monomer from residual MEHQ and peroxides.<sup>†</sup>

The vacuum apparatus is setup as shown in fig 2.2, which consists of (1) a boiling flask containing a small portion (~1g) of CaH<sub>2</sub> and some boiling chips, (2) a thermometer, (3) a liebig condenser, (4) 2 collection flasks which are

---

<sup>†</sup> Reaction between dissolved oxygen and methacrylate monomers during storage yields methacrylate peroxides, which spontaneously decompose by a thermally activated mechanism to yield radical species that act to initiate / terminate the polymerisation of the monomer. [Nising, P., Meyer, T., Carloff, R., Wicker, M., *Macromolecular Materials and Engineering*, 2005. **290**: p. 311.]

Distillation is performed in vacuo to remove dissolved oxygen and lower the monomers boiling point, so as to prevent autopolymerisation and decomposition of peroxides.

attached to a rotating 4-prong adapter (5) and Teflon taps at the nitrogen/vacuum inlets and outlets. The still is purged/backfilled with nitrogen 3 times before being placed under a positive pressure of nitrogen with an oil bubbler based pressure relief valve.

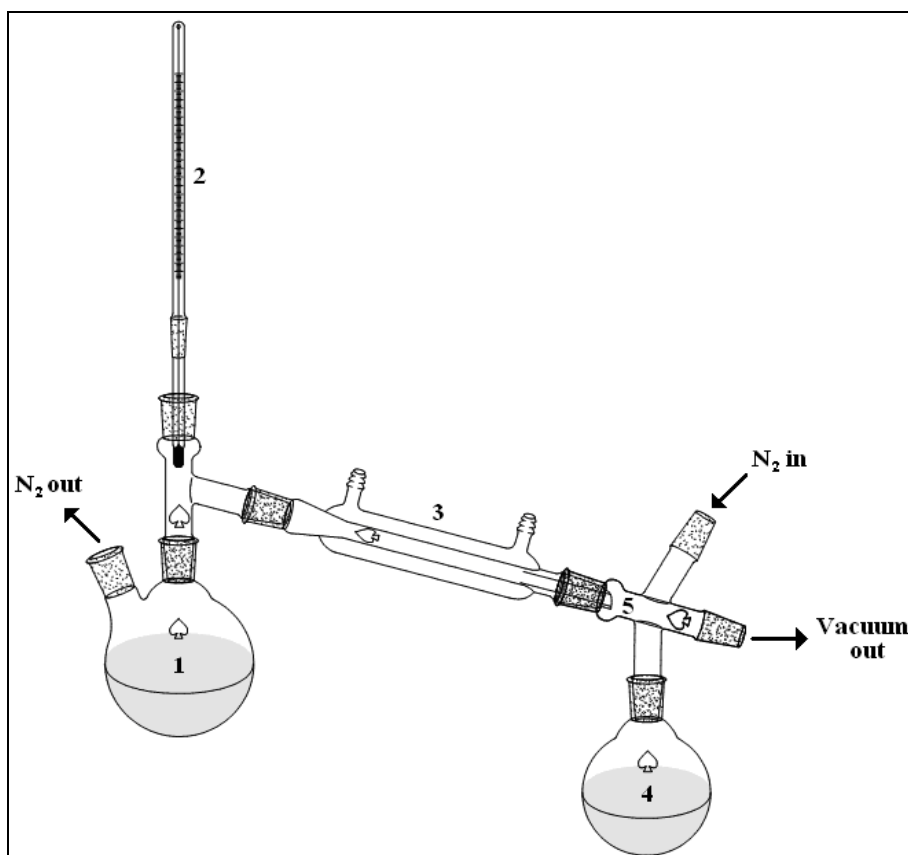


**Fig 2.2:** Vacuum distillation apparatus setup during nitrogen purging.

The dried monomer is eluted through the alumina directly into the vacuum apparatus by connecting a glass column (6) to the still by replacing one of the Teflon taps as shown in fig 2.3. This column is purged under a positive pressure of nitrogen (from (7)) for ~10 min and is then connected to a T shaped gas inlet (8) through which nitrogen is admitted. A small piece of cotton wool is then packed into the bottom of the column, which is subsequently loaded with activated basic alumina (Brockmann 1 grade) up to a height of ~15cm.

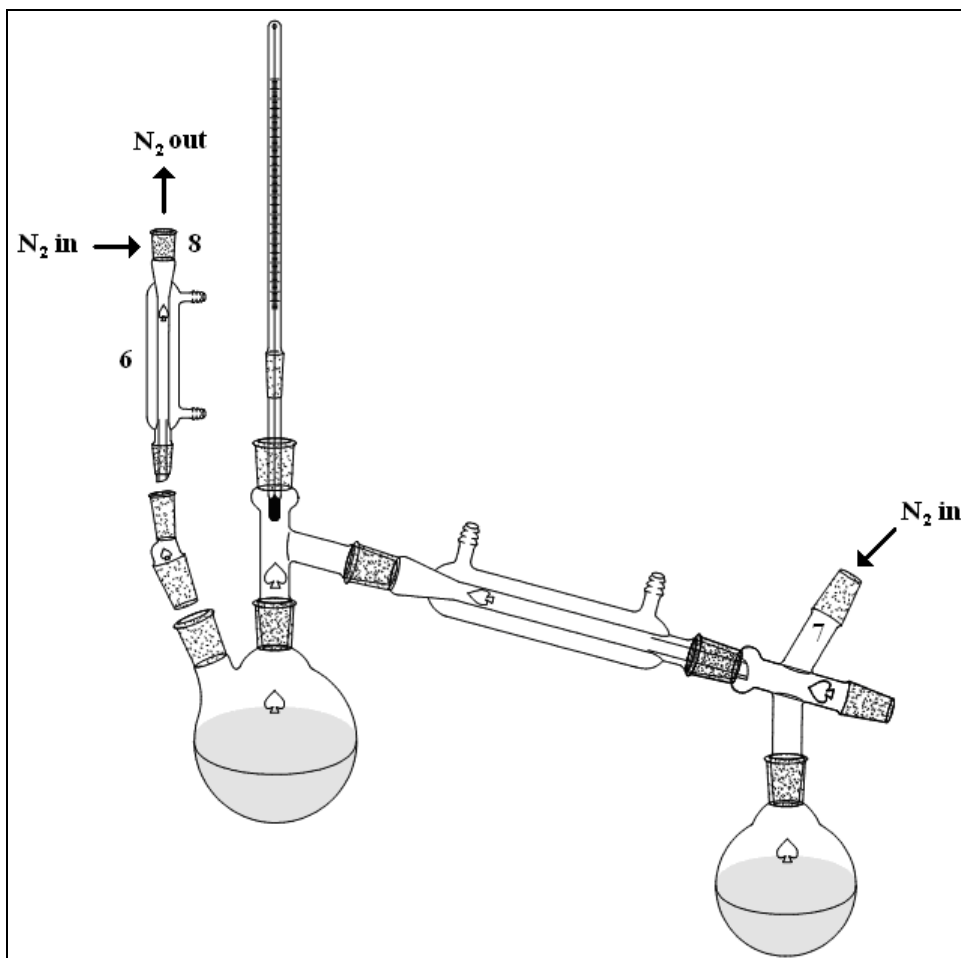


**Fig 2.3:** Vacuum distillation apparatus setup during addition of monomer via elution through an activated alumina column.

The monomer is then eluted through the alumina while the column and still are maintained at a slight positive nitrogen pressure. The column is then removed and replaced with a Teflon tap and the nitrogen inlet and outlets are closed. The monomer is then vacuum distilled by heating the flask to 35°C. The initial 5ml of distillate is collected in one flask attached to the end of the 4-prong adapter, and the adapter rotated so further distillate flows into the other collection flask. Following distillation, the still is slowly repressurised with nitrogen, and the collection flask quickly removed, stoppered with a rubber subbaseal and then purged with nitrogen for 5 minutes to ensure no oxygen is present in the flask. The distilled methacrylate is then either used immediately or stored in a freezer (~ -15°C) for at most 24 hours before use.

### Catalyst Purification

Cu(I) halides, CuBr (Aldrich, 99.999%) or CuCl (Aldrich, 99.995%), are purified (separated from Cu(II) halides) by stirring 200-250mg of either solid with glacial acetic acid (30 ml) for 24 hours, followed by washing consecutively with glacial acetic acid, ethanol and diethyl ether. The resulting solid is then dried at 40°C for 3 days and stored under a nitrogen atmosphere until use. [56]

### PMMA-Br Macroinitiator Synthesis

In a typical PMMA macroinitiator preparation, the mole ratio of [MMA] : [EBrIB] : [CuBr] : [PMDETA] used is 474 : 1 : 1 : 1, which is equivalent to a mass ratio of 1 : 0.00411 : 0.00302 : 0.00365. The following procedure uses example quantities that are scaled accordingly.

CuBr (11.4mg, 0.08mmol) is added to a round bottom flask (designated as the reaction vessel) along with a magnetic stir bar. The flask is stoppered with a subaseal, and the vessel is purged with nitrogen for at least ½ hour, after which it is maintained under a nitrogen atmosphere. Following this, separate solutions of PMDETA (Aldrich, 99%) (6.89mg/ml or 0.04mmol/ml) and EBrIB (Aldrich, 98%) (7.756mg/ml or 0.04mmol/ml) are made up with 25ml Methoxybenzene (Aldrich 99.7%), and the flasks stoppered with subaseals. The MMA (200ml), PMDETA and EBrIB solutions are then deoxygenated by bubbling with nitrogen gas for 1 hour, after which they are maintained under a nitrogen atmosphere. MMA (4ml, 37.55mmol) is then removed from the sealed monomer flask using a nitrogen purged, gas-tight syringe and added to the reaction vessel. 2ml of PMDETA solution is then added to the reaction vessel in the same manner and the solution stirred until the CuBr is completely dissolved, yielding a homogeneous pale green solution. The nitrogen inlet is then closed, and 2ml of EBrIB solution is added to the reaction vessel using a nitrogen purged, gas-tight syringe. The reaction vessel is then immediately placed into a temperature controlled oil bath that has been pre-heated to 90°C, and the polymerisation allowed to proceed with stirring

for the desired period of time. To halt the polymerisation, the reaction vessel is removed from the oil bath and rapidly cooled under a stream of cold water. The subseal is then removed to expose the reaction mixture to air, thus irreversibly oxidising the catalyst complex and preventing any further activation of the dormant PMMA-Br species.

The majority of the copper catalyst is removed from the polymer solution by adding to a 10 fold excess of cold methanol (Ajax, analytic grade), in which the polymer precipitates. The polymer is then collected by filtration, and dried in a vacuum oven for 3 days at 40°C under high vacuum. The remaining traces of copper catalyst may then be removed by eluting a dilute solution of the polymer in THF (Chem-Supply, analytic grade) (1.7 g/100ml) through a short column (1.5 - 2cm) of Brockmann 1 grade neutral alumina. ‡ The polymer is then collected by re-precipitating in cold methanol as described above.

For kinetics studies (where accurate polymer yields need to be determined), elution of the polymer solution through neutral alumina is not undertaken so as to prevent loss of polymer that occurs during this step. Although some copper catalyst remains, this mass is insignificant compared to that of the polymer. However, these traces of oxidised copper catalyst do make such samples unsuitable for use as macroinitiators in chain extension polymerisations.

#### PMMA-*b*-PBMA Synthesis

In a typical PMMA-*b*-PBMA chain extension, the mole ratio of [nBMA] : [PMMA-Br] : [CuCl] : [PMDETA] used is 1680 : 1 : 1 : 1, which is equivalent to a mass ratio of 8.936 :  $\phi$  : 0.00042 : 0.00073, where  $\phi$  depends on the molecular weight of the macroinitiator. The following procedure uses example quantities that are scaled accordingly, using a macroinitiator molecular weight of 20000g/mol.

---

‡ Neutral alumina is used to preserve the polymer halide end functionality, so the polymer can act as a macroinitiator in chain extension by ATRP.



CuCl (3.7mg, 0.0374mmol) and 0.748g of PMMA-Br (0.0374mmol) macroinitiator is added to a round bottom flask (designated as the reaction vessel) along with a magnetic stir bar. The flask is stoppered with a subseal and purged with nitrogen for at least ½ hour, after which it is maintained under a nitrogen atmosphere. Following this, a solution of PMDETA (0.64975mg/ml or 0.00374mmol/ml) is made up with Methoxybenzene (25ml), and the flask stoppered with a subseal. The nBMA and PMDETA solution are then deoxygenated by bubbling with nitrogen gas for 1 hour, after which they are maintained under a nitrogen atmosphere. 10ml of PMDETA solution is then added to the reaction vessel using a nitrogen purged, gas-tight syringe and the solution stirred until the CuCl is completely dissolved, yielding a homogeneous pale green solution. The nitrogen inlet is then closed, and nBMA (10ml, 62.8mmol) is added to the reaction vessel using a nitrogen purged, gas-tight syringe. The reaction vessel is then immediately placed into a temperature controlled oil bath that has been pre-heated to 90°C, and the polymerisation allowed to proceed with stirring for the desired period of time. To halt the polymerisation, the reaction vessel is removed from the oil bath and rapidly cooled under a stream of cold water. The subseal is then removed to expose the reaction mixture to air, thus irreversibly oxidising the catalyst complex and preventing any further activation of the dormant PMMA-b-PBMA-Cl species.

Removal of the copper catalyst from the PMMA-b-PBMA polymer solution is performed in the same manner as for the PMMA-Br macroinitiator.

### 2.2.3. Polymer Characterisation

Analysis of the system to determine the extent of termination as a function of monomer conversion is carried out largely by kinetics studies, which involves examination of polymer weight yields as a function of time. Such data is collected through repeated experiments (typically 8 experiments for each reaction time and set of reaction conditions to account for variations due to terminations resulting from the presence of residual oxygen and other

impurities) to ensure the accuracy and reproducibility of the results. These samples are further characterised by Gel Permeation Chromatography (GPC) and Proton Nuclear Magnetic Resonance ( $H^1$ -NMR) spectroscopy to determine the molecular weight / polydispersity and molecular structure of the samples respectively.

#### Gravimetric Analysis

Polymer mass yield (and therefore monomer conversion) was determined gravimetrically by comparing the mass of monomer used in the reaction to the mass of the resulting polymer solid after purification and drying.

#### Molecular Weight

GPC was performed by Polymer Labs (UK) to determine the number averaged molecular weight ( $M_n$ ) and weight averaged molecular weight ( $M_w$ ) of the polymer chains, and therefore the degree of polydispersity (as quantified by the polydispersity index or PDI).

$$PDI = \frac{M_n}{M_w}$$

Degassed THF (stabilised with 250ppm of butylated hydroxytoluene) was used as the eluent at a flow rate of 1ml/min. Dilute polymer samples (2% w/w) in THF were prepared and injected (100 $\mu$ l) for analysis. Calibration was performed using PMMA standards. The absolute molecular weight of PBMA (rather than molecular weight relative to PMMA) at different elution times was determined from GPC data using Benoit's universal calibration equation combined with the Mark-Houwink-Kuhn-Sakurada empirical relation: [63]

$$[\eta]_{PMMA} \cdot M_{Rel} = [\eta]_{PBMA} \cdot M_{Abs}$$

$$[\eta] = K \cdot M^\alpha$$

$$\therefore M_{Abs} = \left( \frac{K_{PMMA}}{K_{PBMA}} M_{Rel}^{1+\alpha_{PMMA}} \right)^{\frac{1}{\alpha_{PBMA}+1}}$$

Where  $M_{Rel}$  is the apparent molecular weight of PBMA relative to PMMA,  $M_{Abs}$  is the actual molecular weight of the PBMA and  $K$  and  $\alpha$  are the Mark-Houwink parameters for PMMA and PBMA polymers in a given solvent. The Mark-Houwink parameters for these polymers in THF at 30°C is given in table 2.2.

**Table 2.2:** Mark-Houwink parameters for PMMA and PBMA in THF at 30°C. [63-65]

Polymer	K (10 <sup>5</sup> dL·g <sup>-1</sup> )	$\alpha$
PMMA	7.56	14.8
PBMA	0.731	0.664

### Chemical Structure

<sup>1</sup>H-NMR spectroscopy was carried out on 1mg samples of polymer in deuterated chloroform solution using a Bruker 400MHz NMR at 25°C. Residual chloroform in the solvent is used as the internal standard.

#### 2.2.4. Microphase Separation

In the microphase separation of the block copolymers, thick (> 1µm) film samples are prepared. Thick film samples are targeted as they are relatively sturdy (easy to handle without damage), provide a bulk microphase separation morphology that is relatively unaffected by interfacial boundary conditions and provide a greater cross-sectional area for imaging during characterisation

compared to thin films. However, thick films also require much longer microphase separation times to achieve an equilibrium morphology compared with thin films.

#### Microphase Separation of PS-*b*-P2VP

Microphase separated block copolymer films are prepared using the following literature procedure [11, 14]:

A solution of 6.8mg PS-*b*-P2VP in 0.5ml dichloromethane (1 wt%) is prepared and agitated to completely dissolve the polymer. (Note that THF may be used as a replacement for dichloromethane [13]). An epoxy resin (araldite) block (5mm wide x 15mm long x 3 thick) that is to be used as a substrate for polymer deposition is cleaned by rinsing with ethanol and drying under a stream of nitrogen. The block is then placed into a jar along with two glass sample tubes that are each filled with 1.5ml of dichloromethane. Several drops (~0.25ml) of the polymer solution is then cast onto the epoxy block, and the jar immediately sealed. The resulting epoxy supported polymer film is retained in the jars solvent saturated atmosphere for 7 days, after which the jar is slightly opened (just enough to allow an audible release of pressure) to allow all of the solvent to evaporate over the course of 24 hours. The jar is then completely opened to allow the films to air dry for a further 24 hours, followed by an additional 24 hours of drying in vacuo (<50mbar) at room temperature.

#### Microphase Separation of PMMA-*b*-PBMA

The preparation of microphase separated PMMA-*b*-PBMA films may be performed by following the same procedure as used for PS-*b*-P2VP, except that toluene is used instead of dichloromethane and the films are thermally annealed at 140°C under vacuum for 7 days instead of in vacuo at room temperature for 24 hours. [59, 66-69]

### 2.2.5. Microphase Characterisation

The microphase separation of the block copolymer films is characterised by performing transmission electron microscopy (TEM) upon cross-sections of the polymer samples. This is carried out by the following procedure:

#### Sample Preparation

The epoxy substrate supporting the microphase separated block copolymer is first shaped to provide an end face 0.5mm high and 1mm wide as shown in fig 2.4. The angle between the end face and the cut surfaces is ideally  $\sim 150^\circ$ .

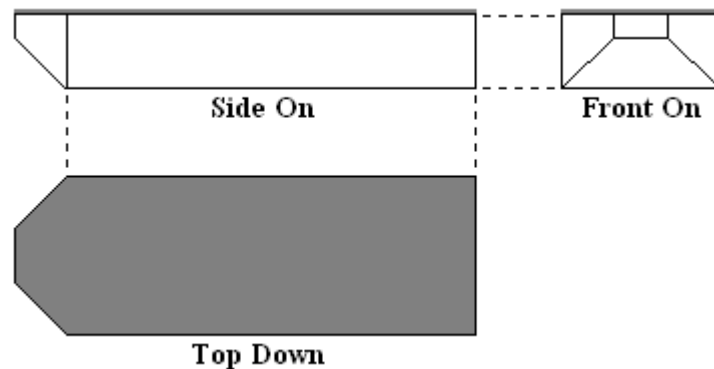


**Fig 2.4:** Depiction of an epoxy substrate coated with a diblock copolymer film that has been shaped to provide a suitable face for ultramicrotomy.

The small end face (and supported polymer film) is then cut into  $\sim 100\text{nm}$  thick cross-sections using a Reichert OMu3 Thermal Advance Ultramicrotome with freshly cut glass knives that have an attached water reservoir that is used to float the cross-sections. Note that room temperature ultramicrotomy can be used in the cross-sectioning of PS-b-P2VP [13] and PMMA-b-PBMA. [59] The sections are then deposited onto a plain Cu TEM grid (200 mesh) by first dipping the grid into a dilute detergent solution (so it will not disturb the water meniscus of the reservoir that the cross-sections are floating on), maneuvering the grid beneath the sections floating on the water

reservoir and then raising the grid to collect them. The grid deposited cross-sections are then allowed to dry in air under a lamp.

### *Imaging*

Before the cross-sections are examined by electron microscopy, they need to be stained in order to enhance the contrast between microphases in the cross-sections. Staining is performed by exposing the cross-sections to the vapour of a high electron density substance that permeates the sections and selectively reacts with one of the polymer blocks. The consequential increase in electron density of the stained microphase allows the microphases to be discerned by TEM. In the case of PS-b-P2VP, iodine crystals are used to selectively stain the P2VP microphases [13], whereas RuO<sub>4</sub> solution is used to stain PBMA microphases in PMMA-b-PBMA. [59]

Grids with deposited cross-sections are placed into a glass sample tube along with the staining agent, and the sample tube sealed. The cross-sections are then left in an atmosphere of the staining agent vapour for a period of time (>10 min for RuO<sub>4</sub> and 4 hours for iodine), after which they are removed from the sample tube. Sections are imaged using a Jeol 1200EX TEM with Megaview 3 Digital camera at an accelerating voltage of 80kV and a spot size of 3.

## 2.3. Results and Discussion

### 2.3.1. PMMA Macroinitiator

#### Synthesis

In order to study the effectiveness of the optimisation of the polymerisation system (determine the monomer conversion at which termination occurs and the nature of such termination), three sets of reproducible data were collected and analysed. The first data set covers the kinetics of the polymerisation.

The rate equation for a well controlled living radical polymerisation is given by the following equation: [22]

$$R_p = \frac{-d[M]}{dt} = k_p[P^*][M]$$

Where  $R_p$  is the polymerisation rate,  $k_p$  is the propagation rate constant,  $[P^*]$  is the concentration of propagating polymer radicals and  $[M]$  is the monomer concentration at a given reaction time. This equation may be further simplified to yield the following:

$$\ln \frac{[M]_o}{[M]} = k_p[P^*]t$$

Where  $[M]_o$  is the initial monomer concentration and  $t$  is time. In the case of a well controlled polymerisation, a plot of  $\ln[M]_o/[M]$  over time will be linear, meaning that the concentration of active growing polymer radicals  $[P^*]$  is constant. A curve with decreasing slope in such a plot suggests that there is a decreasing concentration of polymer radicals over time, which would result from either termination of the growing radical chains or poisoning of the catalyst, which would reduce the number of dormant radicals being

reactivated. [22] By examining such data, the monomer conversions at which the onset of termination occurs may be determined.

Fig 2.5 displays kinetics data for the polymerisation of PMMA macroinitiator in the optimised ATRP system with a monomer/initiator ratio of 474. This data indicates that there is a constant concentration of polymer radicals for the first 30 min (~45% conversion) after which the concentration of such radicals decreases. Given that the decrease in polymer radical concentration occurs quite some time after the reaction has been initiated, that the system is thoroughly degassed and sealed during the reaction and that this result is reproducibly obtained, it is unlikely that poisoning of the catalyst due to impurities (such as oxygen) is responsible for the decrease in polymer radical concentration. Therefore, it is most probable that this result is due to an increase in termination reactions directly involving the polymer radicals.



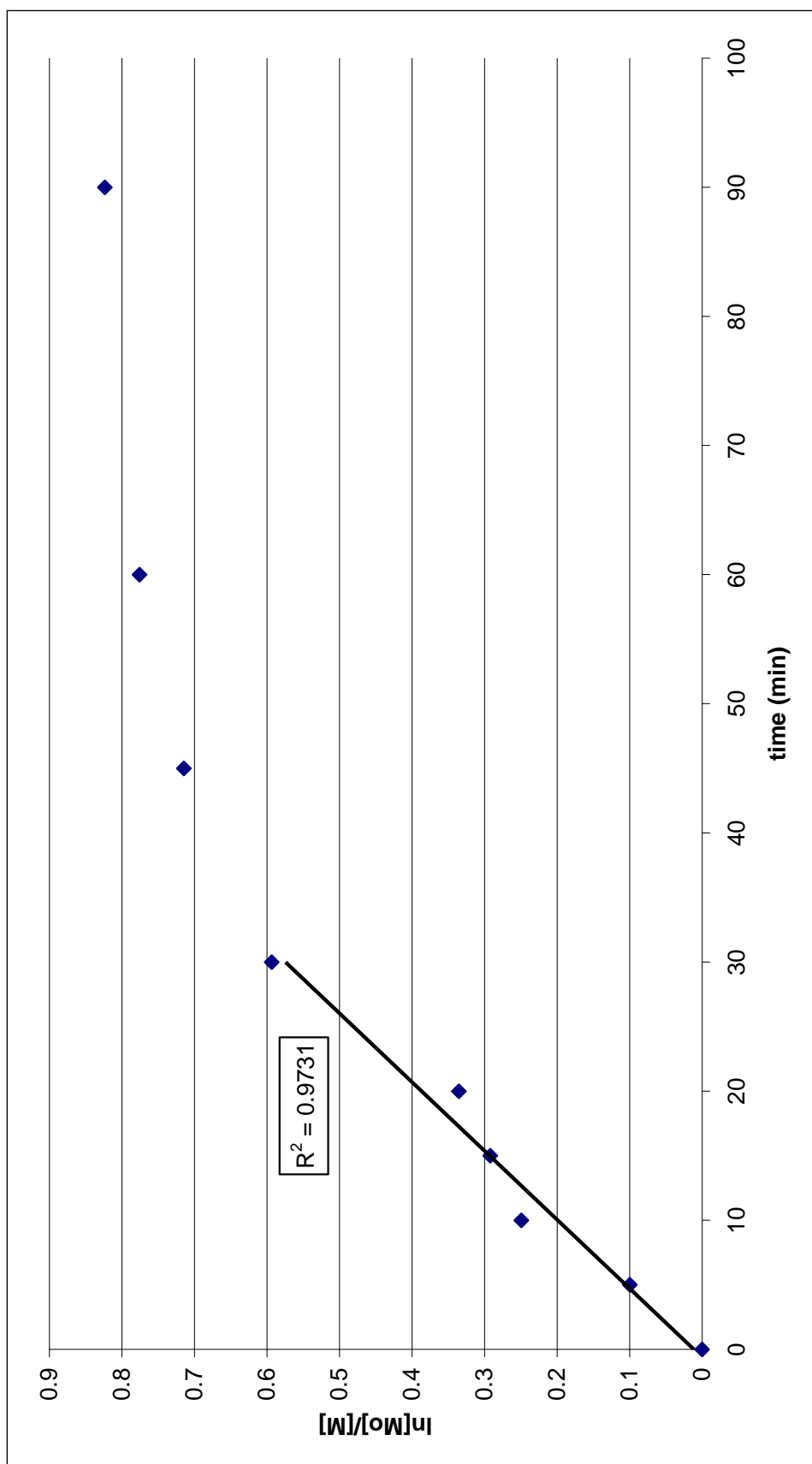


**Fig 2.5:** Kinetic data for the ATRP of PMMA macroinitiator using the CuBr/PMDETA catalyst system and EBrIB as the initiator in 50 vol% methoxybenzene. Each data point is the average of 3 separate polymerisations.

The second set of data examined is the relationship between the number average molecular weight of the polymer chains and monomer conversion, which can be used to determine the form of termination that is dominant. For a controlled radical polymerisation, the number of chains present in the reaction (both active and dormant) should be constant, and therefore, molecular weight should increase linearly with monomer conversion. [22] Thus, for an ideal controlled radical polymerisation, the molecular weight can be predicted from the monomer conversion as described in section 2.1. If termination reactions such as radical chain transfer from active polymer radicals to another species (such as monomer or solvent) or coupling (combination) between propagating polymer radicals occurs, then the number of chains present will increase or decrease respectively. This results in a non-linear change in the number average molecular weight or  $M_n$  with monomer conversion; either a descending curve in the case of chain transfer, or an ascending curve in the case of combination. Note however, that a linear relationship between  $M_n$  and monomer conversion may also be observed if termination by disproportionation occurs, as the number of chains remains the same. This result can be differentiated from the ideal case by examining this data within the context of kinetic data, which concerns only the number of active polymer chains.

The relationship between number average molecular weight and monomer conversion for the optimised PMMA macroinitiator synthesis is described in fig 2.6. The plotted data exhibits two key features. Firstly, the data exhibits an essentially linear relationship up until monomer conversions beyond 45%, after which there is a downturn in the plotted data. This indicates that chain transfer begins to come into play at this point. Secondly, the measured  $M_n$  are higher than the theoretical  $M_n$ , indicating that the initiation efficiency of the polymerisation is lower than optimal ( $M_{n_{theo}}/M_{n_{gpc}} = 0.7$ ). This likely arises due to early termination of some of the initiator radicals before chain growth can commence.

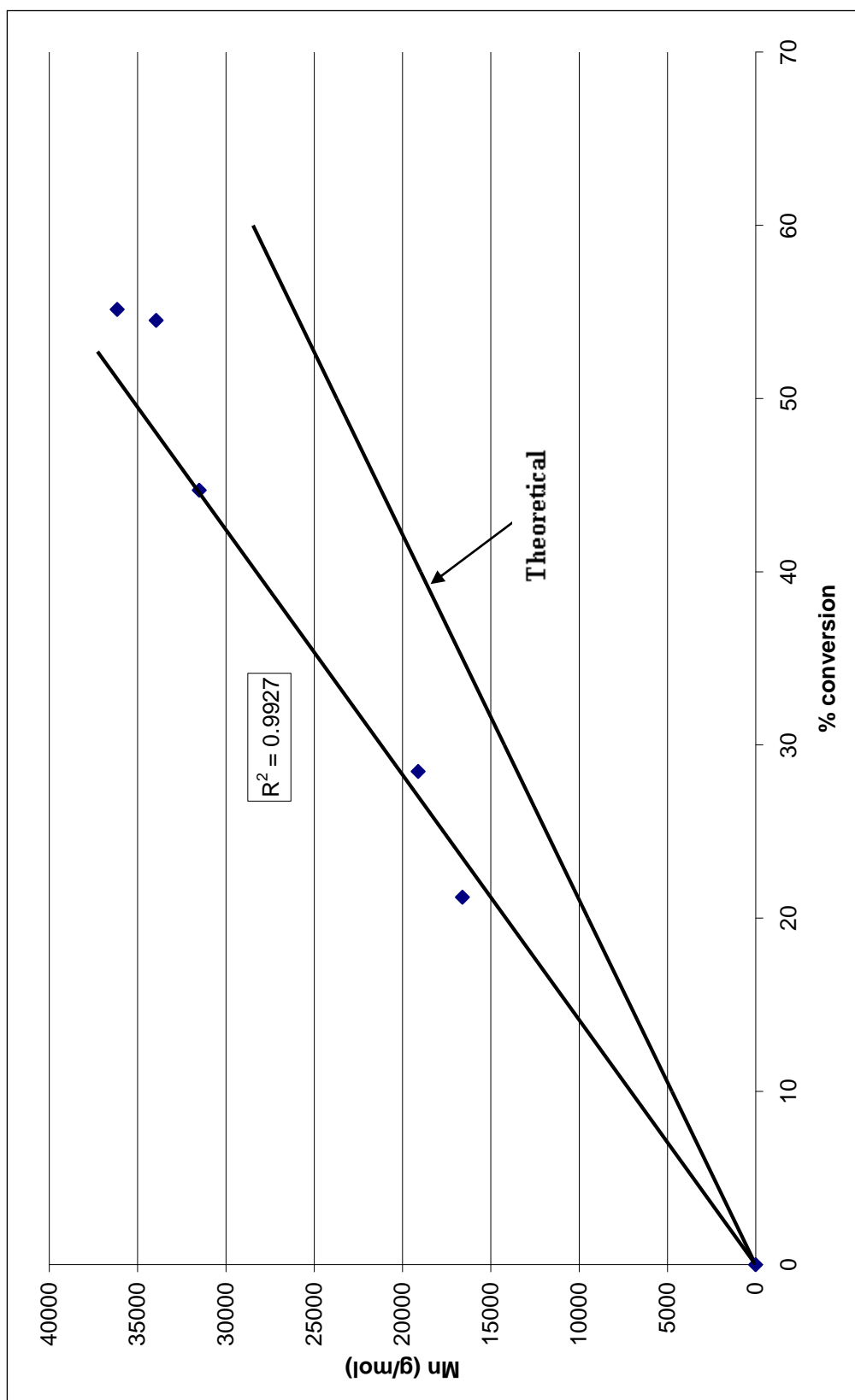


**Fig 2.6:** Molecular weight as a function of monomer conversion for the ATRP of PMMA macroinitiator using the CuBr/PMDETA catalyst system and EBrIB as the initiator in 50 vol% methoxybenzene. Each data point is the average of 3 separate polymerisations.

The last set of data examined is the molecular weight distribution of the PMMA macroinitiator samples prepared at different reaction times. This data was examined in order to determine the extent to which termination reactions occur in this system. In general, a polymerisation is considered to be controlled i.e. has a small distribution of molecular weights, if it has a PDI of  $\leq 1.5$ . As can be seen in fig 2.7, the data suggests that the polydispersity of the polymer remains low ( $\sim 1.15$ ) up until the onset of termination reactions, after which the polydispersity begins to rapidly increase. It is also observed that as the polymer molecular weight increases, a low molecular weight tail develops in the molecular weight distributions, supporting the notion that chain transfer is the dominant termination mechanism.

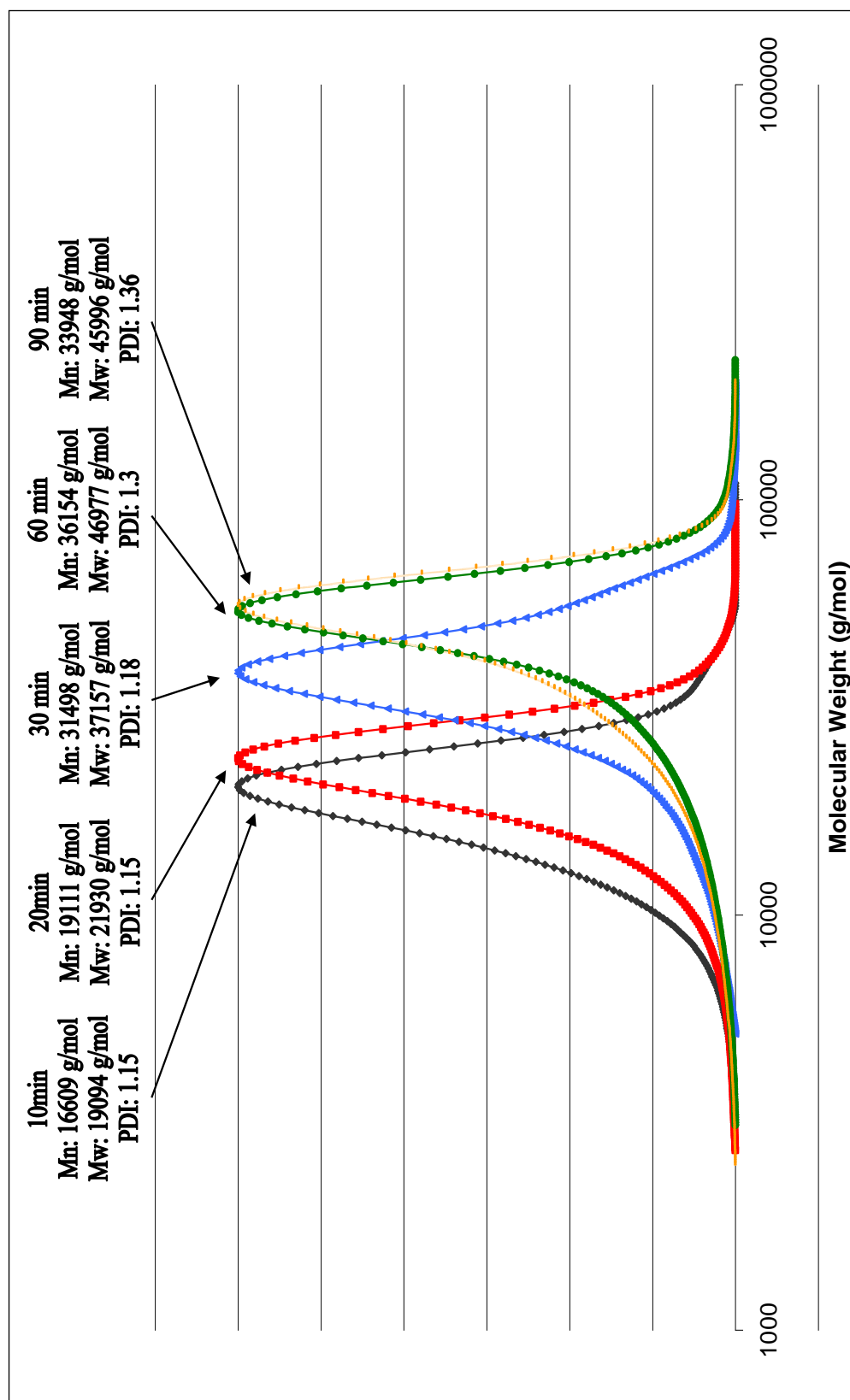


**Fig 2.7:** Molecular weight distribution as determined by GPC for PMMA macroinitiator samples prepared by ATRP using the CuBr/PMDETA catalyst system and EBrIB as the initiator in 50 vol% methoxybenzene.

### Macroinitiator Characterisation

Characterisation of well controlled macroinitiator samples ( $M_n$ : 23800 g/mol, PDI: 1.16) is performed by  $H^1$ -NMR to confirm the chemical composition of the purified polymer (fig 2.8). The acquired spectrum shows large signals due to protons in the polymer chain repeat units (**d**, **e** and **f** in fig 2.8) along with signals due to protons in the EBrIB initiator species (methyl protons at **a** and **c** as well as methylene protons at **b** in fig 2.8) which is incorporated into the polymer. The small signal at a chemical shift centred on 3.781ppm is ascribed to pendant methyl ester protons adjacent to the terminal Br end group (**g** in fig 2.8). Overall, this spectrum closely matches that which is reported in the literature. [39, 70] with the exception of the peak at 1.56ppm, which is ascribed to water in the deuterated chloroform solvent and a very small peak at 3.414ppm, which is ascribed to residual methanol. [71] Interestingly, the ratio of integrals for peaks unique to the monomer (**f**) and terminal Br methacrylate units (**g**), after accounting for the overlap of the **f** peak carbon satellite with the **g** peak, is 163.79. Compared with the expected ratio from the molecular weight measured by GPC (273.64), this indicates that only 68.9% of the polymer chains possess Br end groups; a ratio that is unity in the case of an ideal polymerisation (all living polymer chains retain Br end groups). This lower value is largely attributed to lowered end functionality through purification, as termination is not appreciable for this sample (as affirmed by its low polydispersity).

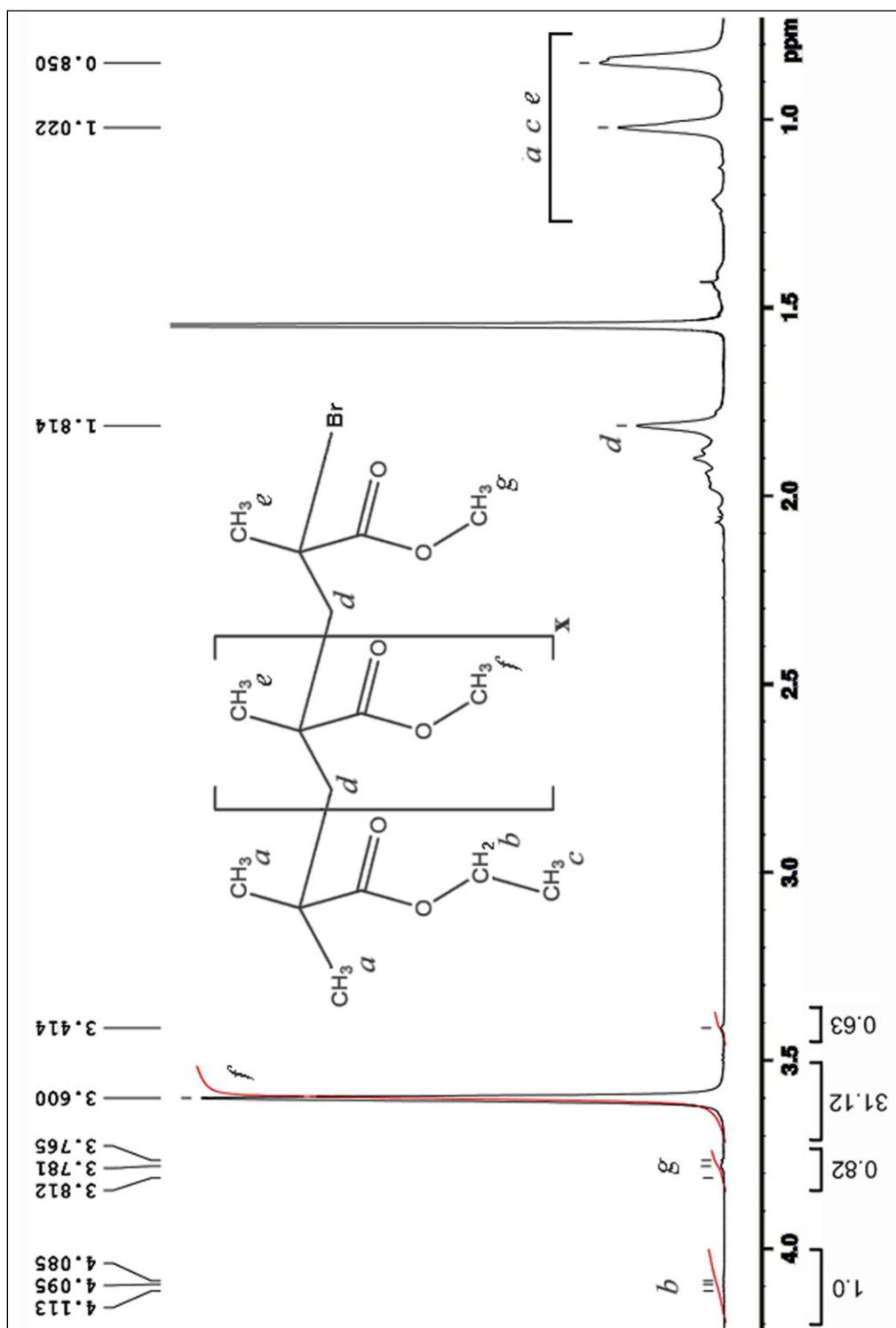


Fig 2.8:  $^1\text{H}$ -NMR spectrum of PMMA-Br macroinitiator.

The non-ideal end functionality of the macroinitiator was further investigated by carrying out a trial chain extension reaction with n-butyl methacrylate or nBMA (monomer/initiator ratio of 1680) using the CuCl/PMDETA catalyst system and a 1 hour reaction time (monomer conversion of 10.85%). GPC results (fig 2.9) for the collected polymer yield a bimodal distribution of molecular weight; a lower molecular weight peak that closely corresponds to that of the macroinitiator, and a high molecular weight peak which is ascribed to PMMA-b-PBMA with a total number average molecular weight of 130875.4 g/mol and a PDI of 1.2 (quoted molecular weight is estimated by excluding the low molecular weight peak). The chemical identities of the two GPC peaks is confirmed to be that of PMMA macroinitiator and PMMA-b-PBMA block copolymer by  $H^1$ -NMR (fig 2.10), which closely matches literature results. [39] These results support the idea that a significant portion of the macroinitiator has lost end functionality prior to chain extension, but that some of the macroinitiator retains such functionality, and can successfully initiate chain extension with BMA.

Comparison of the results from these two analytical techniques allows for the determination of the amount of macroinitiator that successfully initiated chain extension. From GPC, the block copolymer molecular weight is determined to be (23800)-b-(107000) g/mol, yielding a PMMA molar composition of 24%. On the other hand, comparison of the  $H^1$ -NMR resonance signals for n-butyl methacrylate (-CCH<sub>2</sub> protons of the butyloxy pendant at 3.95ppm) with the resonance signals for the methyl methacrylate (-OCH<sub>3</sub> of the methyloxy pendant 3.6ppm) yields a PMMA molar composition of 42.86% for the entire sample (block copolymer and remnant macroinitiator). From this, ~42.2% of the macroinitiator was calculated to successfully initiate polymerisation. This is somewhat lower than the end functionality determined by  $H^1$ -NMR of the macroinitiator, likely due to imperfect initiation by the macroinitiator which retained end functionality.

Importantly, it is also noted from the GPC results that chain extension proceeded to high molecular weights while retaining a low polydispersity, even at a high monomer to initiator ratio (effectively 3980:1 due to loss of



initiator end functionality) with low monomer conversion. This was ascribed to the halogen exchange during the chain extension polymerisation.



**Fig 2.9:** Molecular weight distribution as determined by GPC of ( $\square$ ) PMMA macroinitiator and ( $\diamond$ ) PMMA-b-PBMA block copolymer prepared using this macroinitiator.

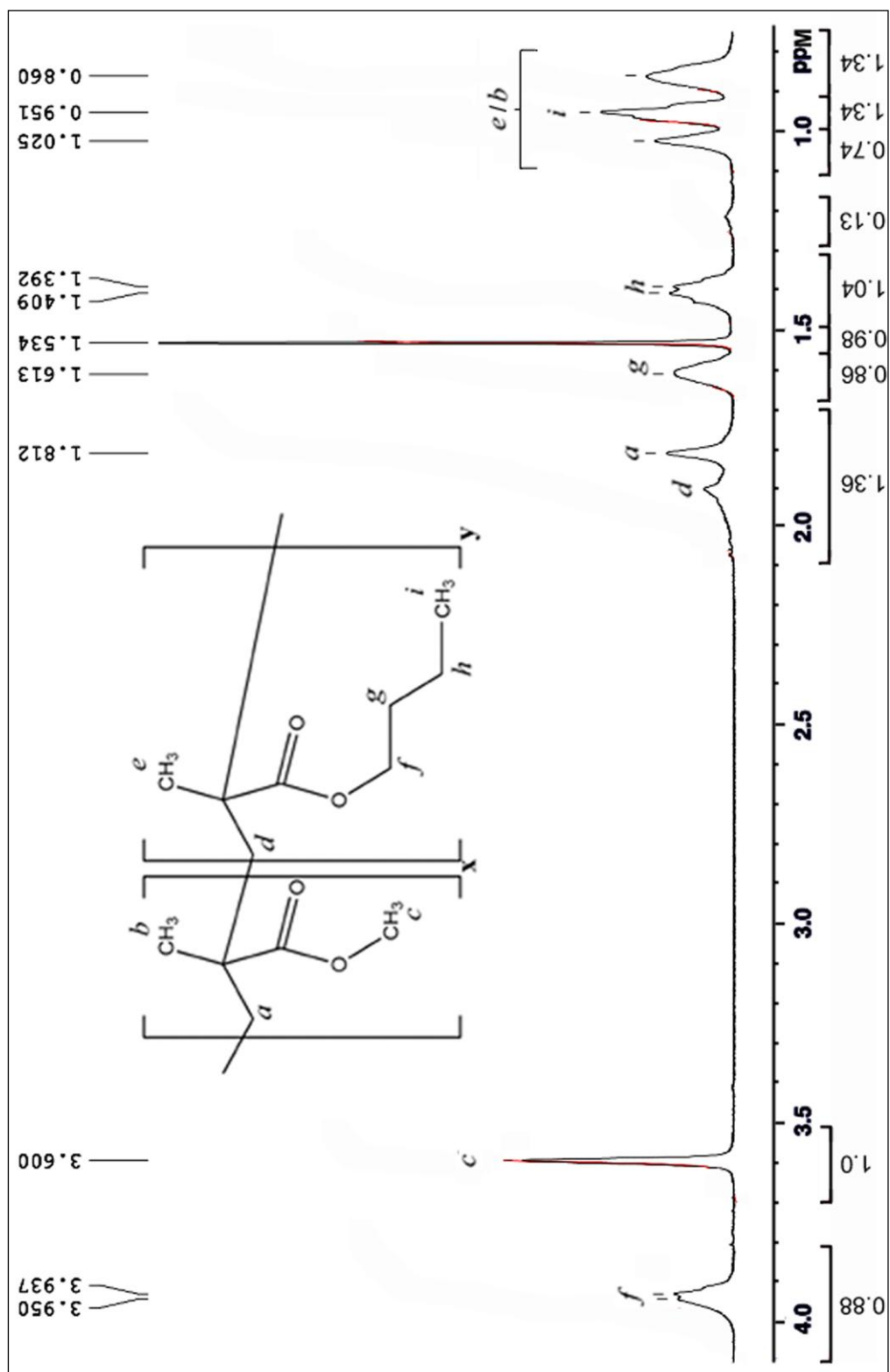


Fig 2.10:  $^1\text{H-NMR}$  of PMMA-*b*-PBMA block copolymer.

### Discussion

The analysis of the macroinitiator polymerisation system indicates that the use of moderate monomer to initiator ratios (effectively 677:1 due to some early termination of the initiator) in the polymerisation of PMMA using the CuBr/PMDETA catalyst system results in termination reactions becoming prevalent at monomer conversions of around 45%, with a concurrent rapid increase in polydispersity. Evidence suggests that this occurs primarily due to chain transfer reactions.

Overall then, this system is not suitable (with regards to this work) for the preparation of the controlled high molecular weight PMMA macroinitiator needed in the subsequent synthesis of PMMA-*b*-PBMA copolymers.

Termination here occurs at relatively low monomer conversions at the moderate monomer/initiator ratios used, which means that attempts to form even higher molecular weight polymers (by increasing the monomer/initiator ratio) are also likely to involve a large number of termination reactions, even if still lower monomer conversions are targeted.

However, it remains possible to further optimise this reaction by reducing the incidence of chain transfer, so that higher monomer conversions may be targeted. Chain transfer from the growing polymer chains may take place with a number of different elements, such as monomer, solvent, impurities (such as terminated initiator) and even other polymer chains (although this typically only occurs at high monomer conversions). Although some of these chain transfer reactions can be minimised through improved purification of reagents and modification of the reaction conditions, some (such as chain transfer to the monomer) are unavoidable, and are characteristic of the polymerisation system. Therefore, a significant amount of work is required to investigate the contribution of these different species towards chain transfer in this system, and to find ways of minimising these side reactions. Even so, it remains possible that this particular system still may not be able to achieve the desired controlled high molecular weight needed.

The characterisation of the macroinitiator also reveals that considerable loss of halogen end functionality occurs, even in the case of samples produced

under conditions that avoid termination (low monomer conversion). When such macroinitiator is then used in chain extension with BMA, significant amounts of PMMA homopolymer remain mixed with the block copolymer product. This then poses a problem with regards to microphase separation (the large volume fraction of homopolymer swelling a copolymer block of equal molecular weight leading to macrophase separation and therefore a disordered morphology). Therefore, preventing this loss of end functionality is required if this macroinitiator is to be used for ATRP chain extension in forming the block copolymers needed as nanoparticle alignment templates.

Considering the significant amount of additional work uncovered, and now required in order to make the PMMA-b-PBMA block copolymers by ATRP needed as templates for nanoparticle alignment, further work in this direction was not carried out and subsequent work focussed on the use of PS-b-P2VP exclusively as a template medium.

### 2.3.2. Microphase Separation

#### PS-b-P2VP lamellar morphology

PS-b-P2VP (190kg/mol - 190kg/mol, PDI: 1.1) was deposited onto an epoxy resin substrate and subjected to an atmosphere of dichloromethane (as per section 2.2.4) in order to acquire a microphase separated block copolymer with a lamellar morphology. Although samples collected for characterisation by TEM are stained after cross-sectioning, one sample was stained before cross-sectioning (after microphase separation), yielding a highly reflective purple coloured polymer film (fig 2.11); indicative of a highly ordered microphase separated block copolymer film. [3]



**Fig 2.11:** Image of an iodine stained, microphase separated PS-b-P2VP film (lamellar morphology) on an epoxy substrate.

TEM images of cross-sections of the epoxy supported block copolymer film (fig 2.12) show that large lamellar microphases are present throughout the polymer film (darker phases are P2VP rich regions) with a high degree of order and alignment that is largely defect free (aligned parallel to substrate

and air interfaces). Significantly, such ordering is observed to extend over several tens of microns, much greater than is generally observed in the literature. [72-74] Comparison of these images with TEM images of the epoxy substrate (fig 2.13) show that these features are unique to the block copolymer film, supporting the idea that they result from microphase separation. The thickness of these lamellar microphases is measured to be in the range of 55 – 75 nm thick (fig 2.14), which compares well with the theoretically predicted microphase size of 61.13 nm (calculated from the degree of polymerisation and the Flory-Huggins interaction parameter of this copolymer). This indicates that equilibrium microphase separation has been achieved. The observation of some local variation in domain thickness within the film is largely ascribed to variations in solvent evaporation rate as a result of variations in film thickness.

Given the presence of large, highly ordered lamellar microphases, this copolymer (treated under the previously defined conditions) is deemed to be suitable for use in cross-phase nanoparticle alignment.

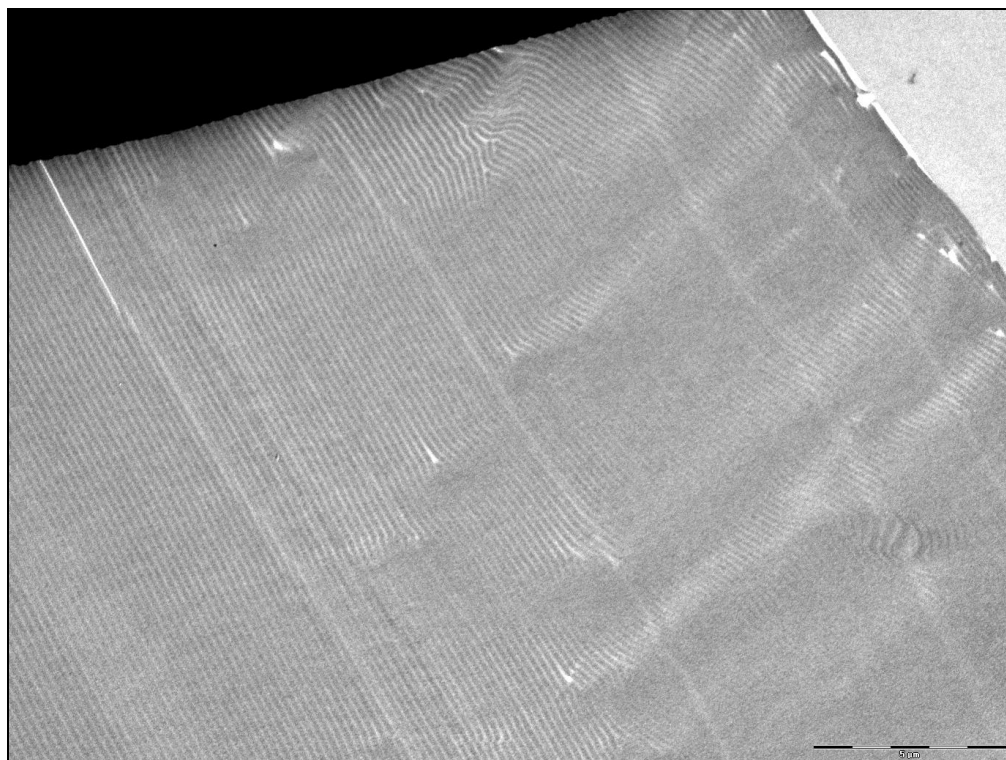


**Fig 2.12:** TEM image of the cross-section of an iodine stained, microphase separated PS-b-P2VP film showing a well ordered lamellar morphology.

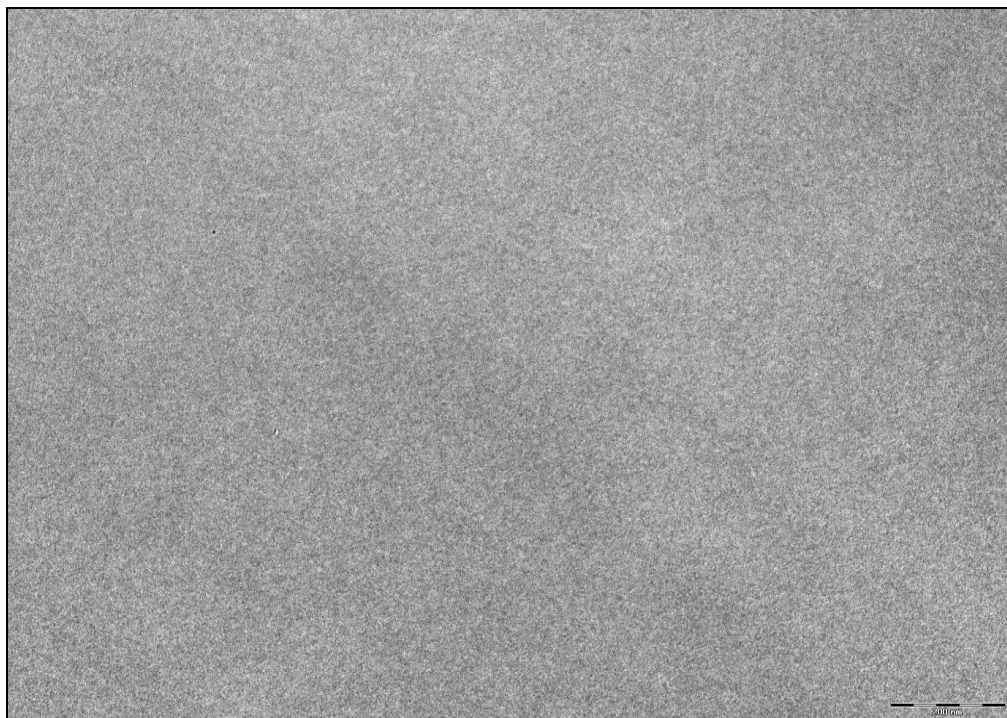


**Fig 2.13:** TEM image of the cross-section of the PS-b-P2VP film's epoxy substrate.



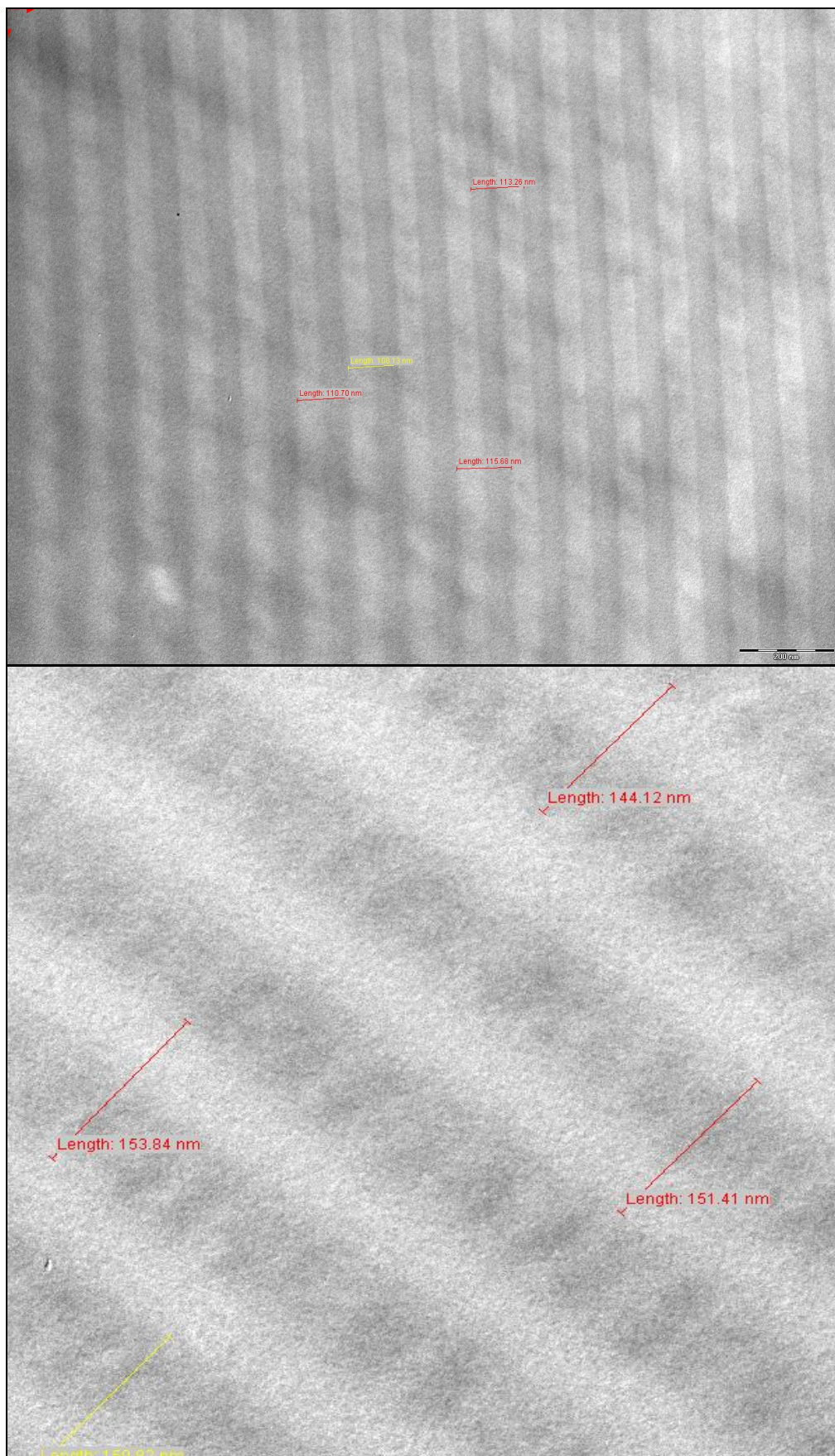


**Fig 2.14:** Close up TEM images of the cross-section of an iodine stained, microphase separated PS-b-P2VP film showing the dimensions of the microphase lamellae.

*PS-b-P2VP spherical morphology*

In the same manner as used to acquire the lamellar morphology, PS-b-P2VP (30kg/mol – 400kg/mol) was deposited onto an epoxy resin substrate and subjected to an atmosphere of dichloromethane (as per section 2.2.4) in order to acquire microphase separated block copolymer with a spherical morphology. Staining of such a microphase separated block copolymer film yields a film noticeably darker red than the epoxy substrate (fig 2.15). This is indicative of a well ordered microphase separation morphology different to that of the lamellar block copolymer.

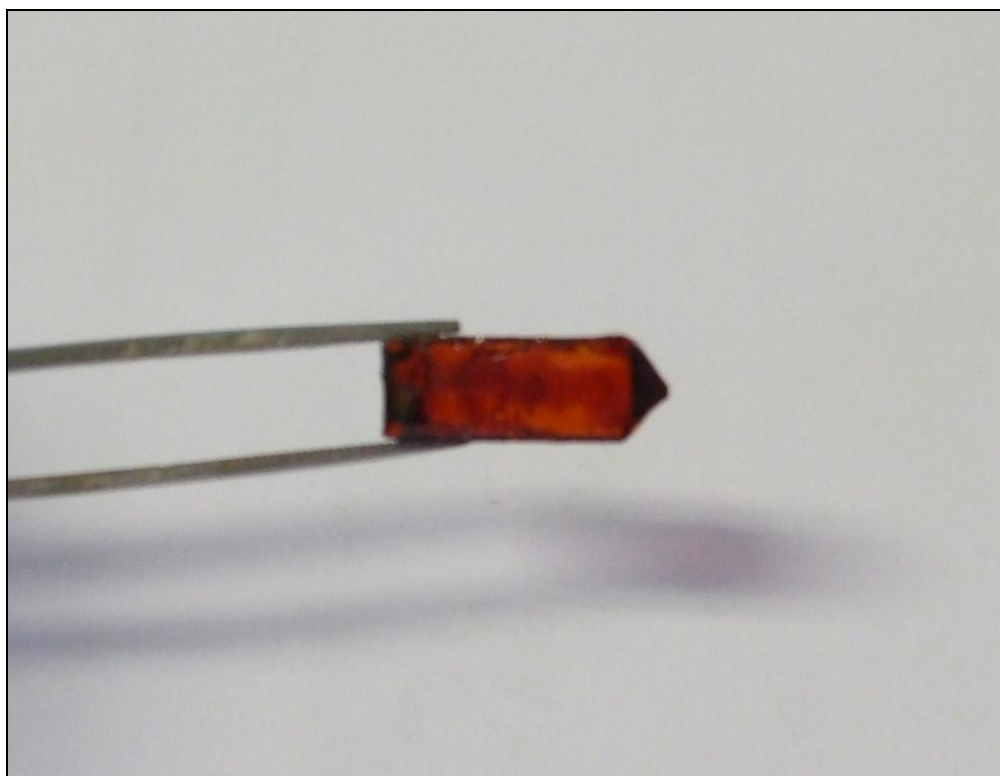


**Fig 2.15:** Image of an iodine stained, microphase separated PS-b-P2VP film (spherical morphology) on an epoxy substrate.

TEM images of cross-sections of the epoxy supported block copolymer film (fig 2.16 and 2.17) exhibit a very well ordered spherical morphology of unstained poly(styrene) spheres in a stained poly(2-vinyl pyridine) matrix, with orientational order extending over length scales of at least 5 microns (generally greater than noted in the literature as before). The diameter of these spheres is measured to be approximately 40nm, significantly less than the

theoretically predicted value of 63.6nm (calculated as described previously). This was largely attributed to their being insufficient time for the block copolymer to attain equilibrium morphology after microphase separation rather than residual solvent acting to shield the repulsive interactions between the blocks, as the observed sharp interfaces between the domains are indicative of strong repulsive interactions.

Given that such spheres meet the minimum anticipated domain size requirement for use in sequestration of the segmented nanorods, this block copolymer (microphase separated under the same conditions for *at least* the same time period) will be used in work involving this block copolymer as a template for nanoparticle alignment.

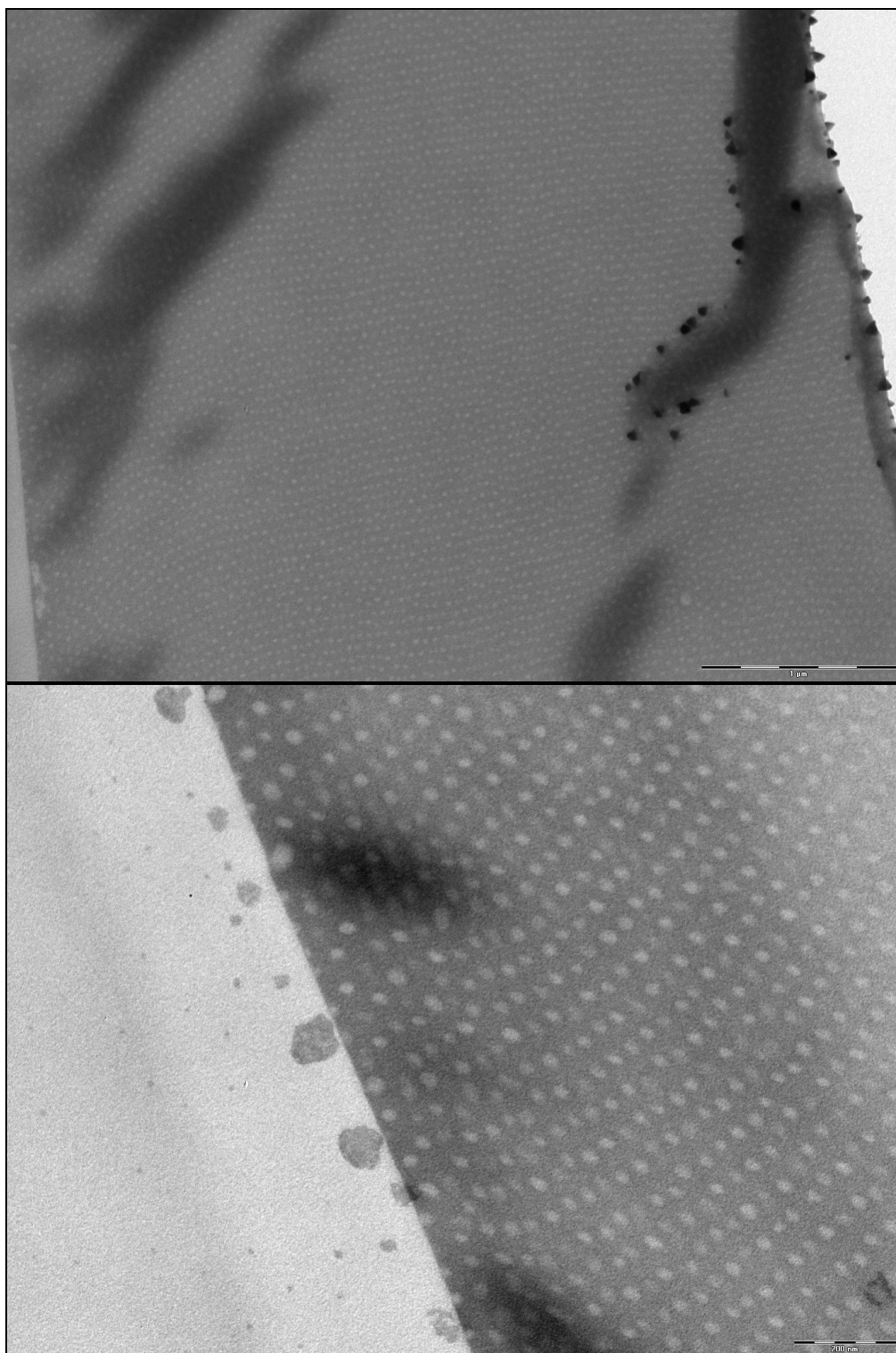


**Fig 2.16:** TEM image of the cross-section of an iodine stained, microphase separated PS-b-P2VP film showing a well ordered spherical morphology.



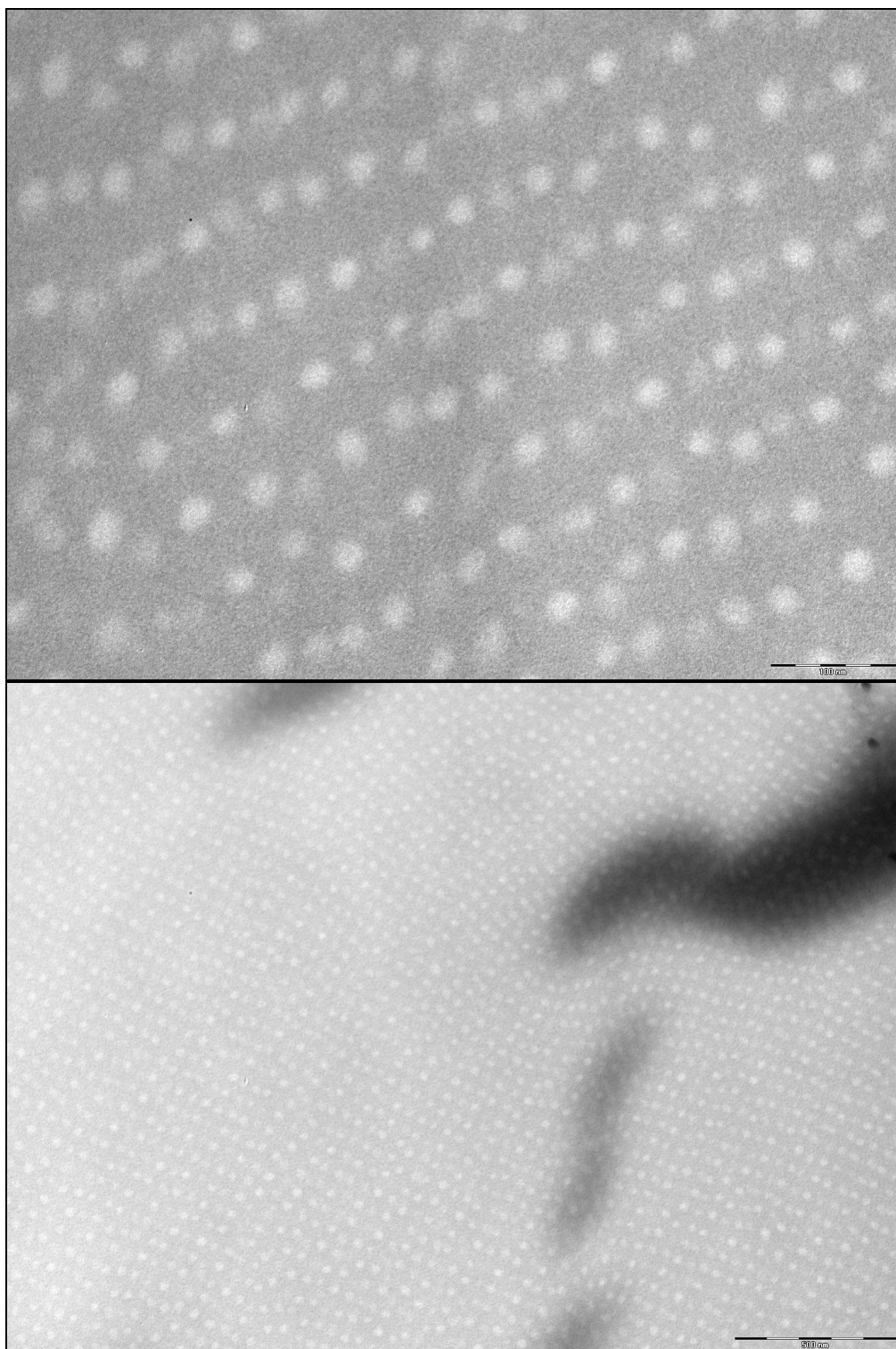


**Fig 2.17:** TEM image of the cross-section of an iodine stained, microphase separated PS-b-P2VP film showing a well ordered spherical morphology.

## 2.4. Conclusions

In conclusion, block copolymer PS-b-P2VP with controlled high molecular weight was obtained and allowed to successfully phase separate to yield well ordered lamellar and spherical microphase morphologies with dimensions sufficiently large to accommodate the segmented nanorods (see next chapter) for template directed alignment. The synthesis of PMMA-b-PBMA was also successfully performed using an ATRP system that is optimised towards high molecular weight and low polydispersity. The targeted controlled high molecular weights are difficult to obtain using this system, as termination by chain transfer occurs at relatively modest combinations of monomer/initiator ratio and monomer conversion. Additionally, a large portion of the PMMA macroinitiator was found to have lost halogen end functionality, meaning that use of this macroinitiator to form a block copolymer will yield a block copolymer mixture containing a significant amount of residual PMMA homopolymer, likely resulting in a disordered morphology. Considering the significant amount of work required to further optimise this ATRP system towards higher controlled molecular weights and improved macroinitiator end functionality, along with the role of this polymer in investigating the template directed alignment of segmented nanoparticles, where it was to be used to examine the effect of microphase interfacial thickness, it is decided that no further work in this direction is to be conducted. As such, studies in this dissertation regarding the template directed alignment of segmented nanorods will exclusively focus on the use of microphase separated PS-b-P2VP templates.

## 2.5. References

1. Lai, C., Russel, W. B., Register, R. A., *Macromolecules*, 2002. **35**: p. 4044.
2. Orso, K.A., Green, P. F., *Macromolecules*, 1999. **32**(4): p. 1087.
3. Urbas, A., Sharp, R., Fink, Y., Thomas, E. L., Xenidou, M., Fetters, L. J., *Advanced Materials*, 2000. **12**(11): p. 812.
4. Meier, D.J., *Polymer Preparation* (American Chemical Society Division of Polymer Chemistry), 1977. **18**: p. 340.
5. Tanaka, H., Hasegawa, H., Hashimoto, T., *Macromolecules*, 1991. **24**: p. 240.
6. Lu, X., Weiss, R. A., *Macromolecules*, 1993. **26**: p. 3615.
7. Mirkin, C.A., Qin, L., Park, S., Huang, L., Chung, S-W., *Multicomponent Nanorods*, USPTO, Editor. 2005, Northwestern University: USA.
8. Natan, M.J., Mallouk, T. E., Martin, B. R., Reiss, B. D., Bietz, L. J., Winkler, J. L., *Method of Manufacture of Colloidal Rod Particles as Nanobarcodes*, USPTO, Editor. 2005, Nanoplex Technologies, Inc.: USA.
9. Hashimoto, T., Shibayama, M., Kawai, H., *Macromolecules*, 1980. **13**: p. 1237.
10. Hashimoto, T., Shibayama, M., Kawai, H., *Macromolecules*, 1980. **13**: p. 1660.
11. Chiu, J.J., Kim, B. J., Kramer, E. J., Pine, D. J., *Journal of the American Chemical Society*, 2005. **127**: p. 5036.
12. Kim, B.J., Bang, J., Hawker, C. J., Kramer, E. J., *Macromolecules*, 2006. **39**: p. 4108.
13. Kim, B.J., Chiu, J. J., Yi, G-R., Pine, D. J., Kramer, E. J., *Advanced Materials*, 2005. **17**: p. 2618.
14. Chiu, J.J., Kim, B. J., Yi, G-R., Bang, J., Kramer, E. J., Pine, D. J., *Macromolecules*, 2007. **40**: p. 3361.
15. Schulz, M.F., Khandpur, A. K., Bates, F. S., Almdal, K., Mortensen, K., Hajduk, D. A., Gruner, S. M., *Macromolecules*, 1996. **29**: p. 2857.

16. Scherble, J., Stark, B., Stuhn, B., Kressler, J., Schubert, D. W., Budde, H., Horing, S., Simon, P., Stamm, M., *Macromolecules*, 1999. **32**: p. 1859.
17. Ballard, D.G.H., Wignall, G. D., Schelten, J., *European Polymer Journal*, 1973. **9**: p. 965.
18. Tangari, C., King, J. S., Summerfield, G. C., *Macromolecules*, 1982. **15**: p. 132.
19. Shull, K.R., Kramer, E. J., Hadziioannou, G., Tang, W., *Macromolecules*, 1990. **23**: p. 4780.
20. Kirste, R.G., *Makromolekulare Chemie*, 1967. **101**: p. 91.
21. Schubert, D.W., Abetz, V., Stamm, S., Hack, T., Siol, W., *Macromolecules*, 1995. **28**: p. 2519.
22. Matyjaszewski, K., Xia, J., *Chemical Reviews*, 2001. **101**: p. 2921.
23. Mao, B.W., Gan, L. H., Gan, Y. Y., *Polymer*, 2006. **47**(9): p. 3017.
24. Patten, T.E., Matyjaszewski, K., *Advanced Materials*, 1998. **10**(12): p. 901.
25. Simms, R.W., Cunningham, M. F., *Macromolecules*, 2007. **40**: p. 860.
26. Xue, L., Agarwal, U. S., Lemstra, P. J., *Macromolecules*, 2002. **35**: p. 8650.
27. Granel, C., Dubois, P., Jerome, R., Teyssie, P., *Macromolecules*, 1996. **29**: p. 8576.
28. Munirasu, S., Dhamodharan, R., *Journal of Polymer Science, A: Polymer Chemistry*, 2004. **42**: p. 1053.
29. Percec, V., Kim, H-J., Barboiu, B., *Macromolecules*, 1997. **30**: p. 6702.
30. de la Fuente, J.L., Fernandez-Sanz, M., Fernandez-Garcia, M., Madruga, E. L., *Macromolecular Chemistry and Physics*, 2001. **202**: p. 2565.
31. Kwiatkowski, P., Jurczak, J., Pietrasik, J., Jakubowski, W., Mueller, L., Matyjaszewski, K., *Macromolecules*, 2008. **41**(4): p. 1067.
32. Matyjaszewski, K., *ACS Symposium Proceedings*, 2000. **768**: p. 2.
33. Keoshkerian, B., Georges, M., MacLeod, P., Kazmaier, P., Lucosi, P., *Polymer Preprints*, 1998. **39**(2): p. 406.



34. Buback, M., Egorov, M., Gilbert, R. G., Kaminsky, V., Olaj, O. F., Russell, G. T., Vana, P., Zifferer, G., *Macromolecular Chemistry and Physics*, 2002. **203**(18): p. 2570.
35. Asano, T., Le Noble, W. J., *Chemical Reviews*, 1978. **78**: p. 407.
36. Beuermann, S., Buback, M., *Progress in Polymer Science*, 2002. **27**: p. 191.
37. Odian, G., *Principles of Polymerization*. 3<sup>rd</sup> ed. 1991, New York: Wiley.
38. Van Eldik, R., Asano, T., Le Noble, W. J., *Chemical Reviews*, 1989. **89**: p. 549.
39. Fernandez-Garcia, M., de la Fuente, J. L., Fernandez-Sanz, M., Madruga, E. L., *Journal of Applied Polymer Science*, 2002. **84**(14): p. 2683.
40. Xia, J., Matyjaszewski, K., *Macromolecules*, 1997. **30**: p. 7697.
41. Davis, K.A., Matyjaszewski, K., *Macromolecules*, 2000. **33**: p. 4039.
42. Shipp, D.A., Wang, J-L., Matyjaszewski, K., *Macromolecules*, 1998. **31**: p. 8005.
43. Matyjaszewski, K., Wang, J. L., Grimaud, T., Shipp, D. A., *Macromolecules*, 1998. **31**: p. 1527.
44. Wang, X.S., Luo, N., Ying, S. K., *Polymer*, 1990. **40**: p. 4157.
45. Davis, K.A., Matyjaszewski, K., *Chinese Journal of Polymer Science*, 2004. **22**(2): p. 195.
46. Matyjaszewski, K., Shipp, D. A., Wang, J. L., Grimaud, T., Patten, T. E., *Macromolecules*, 1998. **31**: p. 6836.
47. Matyjaszewski, K., Coca, S., Gaynor, S. G., Greszta, D., Patten, T. E., Wang, J-S., Xia, J., *Improved processes based on atom (or group) transfer radical polymerization and novel (co)polymers having useful structures and properties*, USPTO, Editor. 1997: International.
48. Matyjaszewski, K., Pintauer, T., Gaynor, S., *Macromolecules*, 2000. **33**: p. 1476.
49. Matyjaszewski, K., Gaynor, S. G., paik, H-J., Pintauer, T., Pyun, J., Qiu, J., Teodorescu, M., Xia, J., Zhang, X., USPTO, Editor. 2000, Carnegie Mellon University: USA.

50. Chatterjee, D.P., Chatterjee, U., Mandal, B. M., *Journal of Polymer Science, A: Polymer Chemistry*, 2004. **42**(17): p. 4132.
51. Ibrahim, K., Lofgren, B., Seppala, J., *European Polymer Journal*, 2003. **39**: p. 939.
52. Xiong, M., Zhang, K., Chen, Y., *European Polymer Journal*, 2008. **44**(11): p. 3835.
53. Ramakrishnan, A., Dhamodharan, R., *Macromolecules*, 2003. **36**: p. 1039.
54. Zhang, W., Zhu, X., Cheng, Z., Zhu, J., *Journal of Applied Polymer Science*, 2007. **106**(1): p. 230.
55. Dayananda, K., Dhamodharan, R., *Journal of Polymer Science, A: Polymer Chemistry*, 2004. **42**(4): p. 902.
56. Karanam, S., Goosens, H., Klumperman, B., Lemstra, P., *Macromolecules*, 2003. **36**: p. 8304.
57. Grimaud, T., Matyjaszewski, K., *Macromolecules*, 1997. **30**: p. 2216.
58. Yoon, J., Lee, W., Thomas, E. L., *Materials Research Society Bulletin*, 2005. **30**: p. 721.
59. Weidisch, R., Michler, G. H., Arnold, M., Fischer, H., *Journal of Material Science*, 2000. **35**: p. 1257.
60. Cavicchi, K.A., Lodge, T. P., *Journal of Polymer Science, B: Polymer Physics*, 2003. **41**: p. 715.
61. Kim, G., Libera, M., *Macromolecules*, 1998. **31**: p. 2569.
62. Nising, P., Meyer, T., Carloff, R., Wicker, M., *Macromolecular Materials and Engineering*, 2005. **290**: p. 311.
63. Gaborieau, M., Graf, R., Spiess, H. W., *Macromolecular Chemistry and Physics*, 2008. **209**: p. 2078.
64. Hutchinson, R.A., Beuermann, S., Paquet Jr, D. A., McMinn, J. H., *Macromolecules*, 1997. **30**: p. 3490.
65. Chen, Y.-J., Li, J., Hadjichristidis, N., Mays, J. W., *Polymer. Bulletin.*, 1993. **30**(5): p. 1436.
66. Hwang, J., Huh, J., Jung, B., Hong, J-M., Park, M., Park, C., *Polymer*, 2005. **46**: p. 9133.
67. Boker, A., *Self Assembly of Block Copolymers in External Fields*. 2002, University of Bayreuth.

68. Lee, S.-H., Char, K., Kim, G., *Macromolecules*, 2000. **33**: p. 7072.
69. Lee, H.H., Jeong, W-Y., Kim, J. K., Ihn, K. J., Kornfield, J. A., Wang, Z-G., Qi, S., *Macromolecules*, 2002. **35**: p. 785.
70. Uegaki, H., Kotani, Y., Kamigaito, M., Sawamoto, M., *Macromolecules*, 1997. **30**: p. 2249.
71. Gottlieb, H.E., Kotlyar, V., Nudelman, A., *Journal of Organic Chemistry*, 1997. **62**: p. 7512.
72. Costanzo, P.J. and F.L. Beyer, *Macromolecules*, 2007. **40**: p. 3996.
73. Segalman, R., Yokohama, H., Kramer, E. J., *Advanced Materials*, 2001. **13**: p. 1152.
74. van Zoelen, W. and G. ten Brinke, *Soft Matter*, 2009. **5**: p. 1568.